THE AMERICAN MINERALOGIST
JOURNAL OF THE MINERALOGICAL SOCIETY OF AMERICA

Vol. 26 AUGUST, 1941 No. 8

THE ATOMIC ARRANGEMENT OF SYLVANITE

GEORGE TUNELL,
Geophysical Laboratory, Carnegie Institution of Washington.

ABSTRACT

The crystal structure of sylvanite has been analyzed by means of Weissenberg photographs and powder diffraction photographs. The dimensions of the unit cell, all determined by purely röntgenographic measurements, are $a_0=8.94$ Å, $b_0=4.48$ Å, $c_0=14.59$ Å, all ± 0.02 Å, and $\beta=145°26' \pm 20'$. The density measured by Palache is 8.16; the corresponding x-ray density is 8.17. The unit cell contains $2AuAgTe_4$, and a small part of the silver atoms required by this ideal formula is replaced by gold atoms. The space-group is C_{2h}^4-P2/c. The seven parameters defining the atomic positions were determined by calculation of the intensities of the diffraction lines of the powder spectrum (which had been rigorously indexed from the single crystal data), and of the diffraction spots of Weissenberg equator photographs of crystals rotating about the a-axis and [201] zone-axis; the positions of the atoms were confirmed by a Fourier projection of the structure on the plane 010 made from a Weissenberg equator photograph taken with the crystal rotating about the b-axis. The gold atoms are situated in (a) 000; $00\frac{1}{2}$, the silver atoms in (e) $0y\frac{1}{4}$; $0\bar{y}\frac{3}{4}$, with $y=0.433$, and the two sets of tellurium atoms in (g) xyz; $\bar{x}\bar{y}\bar{z}$; $\bar{x}, y, \frac{1}{2}-z$; $x, \bar{y}, \frac{1}{2}+z$, with $x_1=0.298$, $y_1=0.031$, $z_1=0.999$, and $x_2=0.277$, $y_2=0.425$, $z_2=0.235$. Each gold atom and each silver atom is surrounded octahedrally by six tellurium atoms, and each tellurium atom is surrounded octahedrally by three tellurium atoms, two gold atoms, and one silver atom, or by three tellurium atoms, two silver atoms, and one gold atom.

INTRODUCTION

The atomic arrangement of sylvanite has been determined in the present investigation by röntgenographic analysis of faceted crystals from Cripple Creek, Colorado,[1] from Săcărâmbu (Nagy-Ág), Transilvania (Siebenbürgen),[2] and from the Buena Mine, Jamestown District, Colorado.[3] The crystals had a metallic luster and steel grey color; their identity was confirmed by measurement on the two-circle reflection goniometer. New crystallographic axes were chosen for use in the structural investigation to conform with the arrangement of the symmetry elements assumed in the "Internationale Tabellen zur Bestimmung von Kristallstrukturen."[4] The axes of Schrauf[5] are not those of a possible unit cell in the structure and for this reason were not retained for purposes of structural analysis. Schrauf's axes are related to the structural axes by the following transformation:

---

[1] Kindly supplied by Professor Charles Palache of Harvard University.

[2] Kindly furnished by Dr. W. F. Foshag of the United States National Museum

[3] Obtained through the kindness of Dr. E. N. Goddard of the United States Geological Survey.

Schrauf to Tunell $\bar{\tfrac{1}{2}}0\tfrac{1}{2}/0\bar{\tfrac{1}{2}}0/100.$[6]

Rotation and Weissenberg equator and layer-line photographs were made with crystals rotating about the *a*-axis, *b*-axis, and [201] zone-axis.[7] Copper K-radiation was used except that a rotation photograph about the *a*-axis was also made with chromium K-radiation and an equator Weissenberg photograph about the [201] zone-axis with molybdenum K-radiation. Powder photographs were made with filtered and unfiltered copper K-radiation. The crystal of which the first Weissenberg photographs were made came from Cripple Creek, Colorado; it was rotated about the *a*-axis, and equator and layer-line Weissenberg photographs were made. The preliminary measurement on the two-circle reflection goniometer showed that it was elongated parallel to the *a*-axis[8] and twinned according to the common law for sylvanite, twinning plane {001},[9] and the graphical construction of the layers of the reciprocal lattice from the Weissenberg photographs by the method of Schneider[10] confirmed the twin-law. A powder photograph with unfiltered copper K-radiation was made of this crystal. Single crystals were obtained from a specimen from Săcărâmbu (Nagy-Ág);[11] one was elongated parallel to the *a*-axis and was bounded by several good faces in the zone parallel to this axis and one cleavage parallel to {010}; this cleavage was the surface along which the crystal had been broken off. The cross section of the crystal perpendicular to the *a*-axis had approximately equal diameters in all directions (about 0.1 mm.). Rotation and equator and layer-line Weissenberg photographs were made with this crystal rotating about the *a*-axis. Another single crystal from the same specimen was elongated parallel to the [201] zone-axis[12] and was approximately equi-dimensional in cross section (about 0.05 mm. in diameter); rotation and equator and layer-line Weissenberg photographs were made with this crystal rotating about the [201] zone-axis. A cleavage fragment from the specimen from

---

[4] Internationale Tabellen zur Bestimmung von Kristallstrukturen, Gebrüder Borntraeger, *Berlin*, p. 101 **(1935).**

[5] *Zeits. Krist.*, **2**, 209–252 (1878).

[6] For the reason for the fractional form see M. A. Peacock: *Am. Mineral.*, **23**, 38 (1938).

[7] All letters and symbols in this paper refer to the structural lattice and the unit cell described in the following section except where a statement is made to the contrary.

[8] This is the $[\bar{1}01]$ zone-axis of Schrauf.

[9] This plane has the symbol {101} when referred to the axes of Schrauf.

[10] *Zeits. Krist.*, **69**, 41–48 (1928).

[11] U. S. National Museum, No. R916.

[12] This is the *c*-axis of Schrauf.

Săcărâmbu (Nagy-Âg) was rotated about the *b*-axis, and a rotation and an equator Weissenberg photograph were obtained; the equator Weissenberg photograph showed that this fragment was twinned with the twinning plane {001}. Powder photographs of a sample from this specimen were made with filtered copper K-radiation. Lastly, a well-developed single crystal from the Buena Mine, Jamestown District, Colorado, was measured completely on the two-circle reflection goniometer; its cross section perpendicular to the *b*-axis is roughly triangular, and the average diameter of this cross section is approximately 0.5 mm. Rotation and Weissenberg equator and layer-line photographs were made with this crystal rotating about the *b*-axis, and a rotation and an equator Weissenberg photograph with the crystal rotating about the [201] zone-axis. A search was made for a smaller crystal that could be rotated about the *b*-axis, but none suitable for this purpose could be found.

DETERMINATION OF THE UNIT CELL AND SPACE-GROUP

The dimensions of the structural unit cell, all determined by purely röntgenographic measurements, are $a_0 = 8.94$ Å, $b_0 = 4.48$ Å, $c_0 = 14.59$ Å, all ±0.02 Å; $\beta = 145°26' \pm 20'$.[13] The volume of the unit cell is accordingly 331.6 Å^3. The chemical analysis of crystallographically studied material from the Cripple Creek District, Colorado, made by Palache[14] corresponds to the composition $(Au, Ag)Te_2$ with an atomic ratio of gold to silver equal to 1.15. The density determined by Palache[15] on three isolated crystals by means of the hydrostatic balance is 8.16. The density computed from the *x*-ray measurements with use of the ideal formula $AuAgTe_4$ is 8.11; if the ratio of gold to silver is taken as 1.15 (corresponding to the analysis of Palache) instead of 1.00 (corresponding to the ideal formula), and if, as appears very probable, the slight excess of gold is the result of replacement of silver atoms by gold atoms in the structure, the *x*-ray density is 8.17. The agreement of the measured density with this calculated density leaves no doubt that the content of the unit cell is $2AuAgTe_4$, and confirms the assumption that the slight excess of gold over that required by the ideal formula and the slight deficiency of silver is the result of replacement of part of the silver atoms by gold atoms. Diffraction effects were obtained on the Weissenberg photographs from the following planes: *u*00, *g*00, 0*u*0, 0*g*0, 00*g*, 0*uu*, 0*ug*, 0*gu*, 0*gg*, *u*0*g*, *g*0*g*, *ug*0, *gu*0, *gg*0, *uu*0,[16] *uuu*, *uug*, *ugu*, *ugg*, *guu*, *gug*, *ggu*, *ggg*, where *u* denotes any odd number and g denotes any even number. No diffraction effects were obtained from the following: $00u$, $u0u$, $g0u$, although representatives of each were in a position to diffract. Thus sylvanite belongs either to the space-group C_s^2-Pc or to the space-group C_{2h}^4-P2/c, both of which are characterized by the absence of diffraction effects from $00u$, $u0u$, and $g0u$, due to the presence of a glide plane parallel to 010 with a glide component of $c/2$. Faceted crystals of sylvanite have been studied with the reflection goniometer by several investigators. Projections of such crystals drawn by Koksharov, Schrauf, Vrba, and Palache and reproduced by V. Goldschmidt in his "Atlas der Krystallformen"[17] show the habit of sylvanite to be holohedral. Morphological study of crystals used in the present röntgenographic investigation also indicates the presence of a two-fold axis and consequently points to holohedral symmetry. Hence the space-group of sylvanite is C_{2h}^4-P2/c.

---

[13] Tunell, G. and Ksanda, C. J.: *Am. Mineral.*, **22**, 728 (1937).

[14] *Am. Jour. Sci.*, (4), **10**, 422 (1900).

[15] *Am. Jour. Sci.*, (4), **10**, 419 (1900).

[16] It was reported previously (*Am. Mineral.*, **22**, 728 (1937)) that no diffraction effects were obtained from planes having indices *uu*0. The statement was based on examination of a Weissenberg photograph of the first layer-line (crystal rotating about the *a*-axis). Since

Determination of the Atomic Arrangement

There are two gold, two silver, and eight tellurium atoms to be located in the unit cell. The space-group C_{2h}^4-P2/c furnishes the following sets of equivalent positions:

(a) $000;\ 00\tfrac{1}{2};$ (b) $\tfrac{1}{2}\tfrac{1}{2}0;\ \tfrac{1}{2}\tfrac{1}{2}\tfrac{1}{2};$ (c) $0\tfrac{1}{2}0;\ 0\tfrac{1}{2}\tfrac{1}{2};$
(d) $\tfrac{1}{2}00;\ \tfrac{1}{2}0\tfrac{1}{2};$ (e) $0y\tfrac{1}{4};\ 0\bar{y}\tfrac{3}{4};$ (f) $\tfrac{1}{2}y\tfrac{1}{4};\ \tfrac{1}{2}\bar{y}\tfrac{3}{4};$
(g) $xyz;\ \bar{x}\bar{y}\bar{z};\ \bar{x},\ y,\ \tfrac{1}{2}-z;\ x,\ \bar{y},\ \tfrac{1}{2}+z;$

of which (a), (b), (c), and (d) have the symmetry C_i, (e) and (f) the symmetry C_2, and (g) the symmetry C_1. Several different arrangements of the atoms in these positions are possible with reasonable interatomic distances. Only one of these arrangements could be found, however, that yields calculated intensities in agreement with those observed. This arrangement is the following: gold atoms in (a) 000, $00\tfrac{1}{2}$; silver atoms in (e) $0y\tfrac{1}{4}$, $0\bar{y}\tfrac{3}{4}$; with $y=0.433$; and two sets of tellurium atoms in (g) xyz; $\bar{x}\bar{y}\bar{z}$; $\bar{x},\ y,\ \tfrac{1}{2}-z$; $x,\ \bar{y},\ \tfrac{1}{2}+z$, with $x_1=0.298$, $y_1=0.031$, $z_1=0.999$, and $x_2=0.277$, $y_2=0.425$, $z_2=0.235$. Orthographic projections of this structure are given in Fig. 1, and a model of the structure is shown in Fig. 2.[18] The intensities calculated[19] from this structure are compared with those observed in Tables I, II, III, and IV. Table I contains the observed and calculated intensities of diffraction lines on a powder photograph taken

---

then a Weissenberg photograph of the third layer-line (crystal rotating about the a-axis) has been made and diffraction effects have been found from planes having indices $uu0$. This does not alter any of the conclusions previously drawn.

[17] Carl Winters Universitätsbuchhandlung, *Heidelberg* (**1922**), Band VIII, Tafeln 65–68.

[18] The author is indebted to Mr. H. A. Schmidt, Jr. for the skillful construction of this model.

[19] The author acknowledges with appreciation the painstaking assistance Mrs. R. P. Tunell has rendered in performing the lengthy calculations.

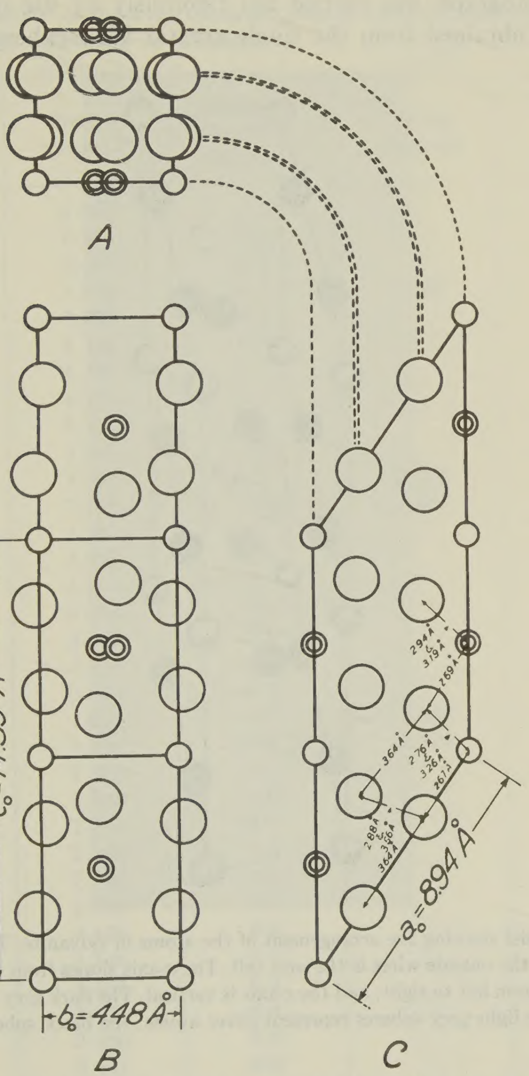

FIG. 1. Orthographic projections of the unit cell of sylvanite. A. Top view. B. Front view. C. Side view. Small single circles—gold atoms. Small double circles—silver atoms. Large circles—tellurium atoms.

with copper K-radiation filtered through nickel foil. The indexing of the powder photograph was carried out rigorously by use of the unit cell dimensions obtained from the single crystal Weissenberg photographs.

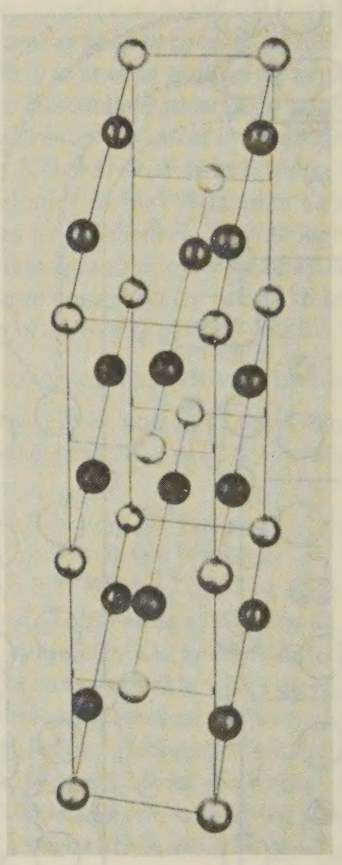

FIG. 2. Model showing the arrangement of the atoms in sylvanite. The parallelepiped represented by the outside wires is the unit cell. The *a*-axis slopes from back to front; the *b*-axis extends from left to right; and the *c*-axis is vertical. The dark grey spheres represent gold atoms; the light grey spheres represent silver atoms; the black spheres represent tellurium atoms.

Table I lists in decreasing order the calculated and observed spacings and intensities of all planes the spacings of which are greater than 1.378 Å, together with the observed spacings and intensities of the remaining lines of the powder photograph. The intensities I_P of the lines on the powder diffraction film taken with filtered radiation were calculated from the formula

$$I_P = \frac{1 + \cos^2 2\theta}{\sin 2\theta} j \,|\, F \,|^2,$$

TABLE I

Relative intensities* of the x-ray diffraction lines of sylvanite from a powder photograph taken with filtered copper K-radiation.

Indices *hkl*	Spacing calculated	Relative intensity calculated	Spacing measured	Relative intensity observed
$10\bar{1}$	8.382	0.0		
001	8.278	0.0		
$10\bar{2}$	7.295	0.2		
100	5.072	0.7	5.102	1
010	4.480	0.2		
$20\bar{3}$	4.408	0.0		
$10\bar{3}$	4.363	0.0		
$20\bar{2}$	4.190	0.1		
002	4.139	0.1		
$11\bar{1}$	3.951	0.0		
011	3.940	0.7	3.970	½
$11\bar{2}$	3.818	0.6	3.851	½
$20\bar{4}$	3.647	0.1		
110	3.358	0.1		
$20\bar{1}$	3.304	0.0		
101	3.285	0.0		
$21\bar{3}$	3.142	0.1		
$11\bar{3}$	3.126	0.0		
$21\bar{2}$	3.060	0.1		
012	3.040	9.9	3.045	10
$30\bar{4}$	2.980	3.9	2.976	6
$10\bar{4}$	2.943	0.1		
$21\bar{4}$	2.828	0.0		
$30\bar{5}$	2.814	0.0		
$30\bar{3}$	2.794	0.0		
$20\bar{5}$	2.794	0.0		
003	2.759	0.0		
$21\bar{1}$	2.659	0.0		
111	2.649	0.1		
200	2.536	0.1		
$31\bar{4}$	2.481	0.1		
$11\bar{4}$	2.460	0.2		
$30\bar{6}$	2.432	0.0		
$30\bar{2}$	2.405	0.0		
102	2.386	0.0		
$31\bar{5}$	2.383	0.3	2.367	½
$21\bar{5}$	2.371	0.0		
$31\bar{3}$	2.370	0.1		
013	2.349	0.3		
020	2.240	2.0	2.244	3
$40\bar{5}$	2.224	0.0		
210	2.207	0.1		

TABLE I—*Continued*

Indices *hkl*	Spacing calculated	Relative intensity calculated	Spacing measured	Relative intensity observed
$40\bar{6}$	2.204	0.0		
$10\bar{5}$	2.195	0.0		
$20\bar{6}$	2.181	0.0		
$12\bar{1}$	2.164	0.1		
021	2.162	0.7		
$12\bar{2}$	2.141	0.1	2.149	5
$31\bar{6}$	2.137	4.1		
$31\bar{2}$	2.122	3.5	2.118	5
112	2.106	0.5		
$40\bar{4}$	2.095	1.2		
004	2.070	2.6	2.076	3
120	2.049	0.3		
$40\bar{7}$	2.047	0.0		
$30\bar{7}$	2.036	0.0		
$30\bar{1}$	2.013	0.0		
201	2.006	0.0		
$22\bar{3}$	1.997	0.0		
$12\bar{3}$	1.993	0.1		
$41\bar{5}$	1.992	0.0		
$41\bar{6}$	1.978	1.7	1.983	4
$22\bar{2}$	1.976	0.0		
$11\bar{5}$	1.971	0.0		
022	1.970	0.3		
$21\bar{6}$	1.961	0.0		
$22\bar{4}$	1.909	0.0		
$41\bar{4}$	1.898	0.0		
$40\bar{3}$	1.881	0.0		
014	1.879	0.1		
103	1.864	0.0		
$41\bar{7}$	1.862	0.1		
$22\bar{1}$	1.854	0.2	1.844	1
$31\bar{7}$	1.854	0.1		
121	1.851	0.0		
$31\bar{1}$	1.836	0.1		
211	1.831	0.0		
$40\bar{8}$	1.824	0.6		
$32\bar{4}$	1.791	1.9	1.796	2
$50\bar{7}$	1.785	0.0		
$12\bar{4}$	1.782	0.1		
$50\bar{6}$	1.767	0.0		
$20\bar{7}$	1.764	0.0		
$32\bar{5}$	1.752	0.2		
$22\bar{5}$	1.748	0.1		
$32\bar{3}$	1.748	0.5		
$10\bar{6}$	1.744	0.1		

TABLE I—*Continued*

Indices *hkl*	Spacing calculated	Relative intensity calculated	Spacing measured	Relative intensity observed
023	1.739	0.4		
$41\bar{3}$	1.735	0.1		
$50\bar{8}$	1.723	0.1	1.727	1 (broad)
113	1.721	0.0		
$30\bar{8}$	1.709	1.5	1.687	
300	1.691	1.0		½
$41\bar{8}$	1.689	0.1		
220	1.679	0.0		
$50\bar{5}$	1.676	0.0		
005	1.656	0.0		
$40\bar{2}$	1.652	0.0		
$51\bar{7}$	1.648	0.0		
$32\bar{6}$	1.648	0.1		
$51\bar{6}$	1.644	0.1		
202	1.642	0.0		
$21\bar{7}$	1.641	0.0		
$32\bar{2}$	1.640	0.2		
122	1.633	0.0		
$11\bar{6}$	1.625	0.0		
$51\bar{8}$	1.608	0.0		
$50\bar{9}$	1.604	0.0		
$40\bar{9}$	1.597	0.0		
$31\bar{8}$	1.597	0.0		
310	1.582	0.1		
$42\bar{5}$	1.578	0.3		
$42\bar{6}$	1.571	0.1		
$51\bar{5}$	1.570	0.0		
$12\bar{5}$	1.568	0.0		
$22\bar{6}$	1.563	0.0		
015	1.553	0.1		
$41\bar{2}$	1.550	1.2		
212	1.542	0.1		
$50\bar{4}$	1.542	0.1		
$42\bar{4}$	1.530	0.8	1.524	
104	1.526	0.2		3
024	1.520	1.7		
$42\bar{7}$	1.511	0.0		
$51\bar{9}$	1.510	0.0		
$32\bar{7}$	1.507	0.4		
$41\bar{9}$	1.505	0.0		
$32\bar{1}$	1.497	0.1		
221	1.494	0.0		
030	1.493	0.2	1.494	½
$60\bar{8}$	1.490	0.3		
$20\bar{8}$	1.472	0.0		

TABLE I—*Continued*

Indices *hkl*	Spacing calculated	Relative intensity calculated	Spacing measured	Relative intensity observed
$13\bar{1}$	1.470	0.0		
031	1.470	0.5		
$60\bar{9}$	1.469	0.0		
$60\bar{7}$	1.464	0.0		
$13\bar{2}$	1.463	0.1		
$5.0.\overline{10}$	1.459	0.0		
$51\bar{4}$	1.458	0.0		
$30\bar{9}$	1.454	0.0		
114	1.445	0.0		
$10\bar{7}$	1.444	0.0		
$40\bar{1}$	1.444	0.0		
$42\bar{3}$	1.441	0.0		
301	1.440	0.0		
123	1.433	0.1		
130	1.432	0.0		
$23\bar{3}$	1.414	0.1	1.413	1 (broad)
$42\bar{8}$	1.414	0.5		
$61\bar{8}$	1.414	0.0		
$13\bar{3}$	1.413	0.1		
$6.0.\overline{10}$	1.407	0.0		
$23\bar{2}$	1.407	0.0		
032	1.405	0.6		
$21\bar{8}$	1.398	0.0		
$4.0.\overline{10}$	1.397	0.1		
$60\bar{6}$	1.397	0.0		
$61\bar{9}$	1.396	0.0		
$52\bar{7}$	1.396	0.0		
$50\bar{3}$	1.394	0.0		
$61\bar{7}$	1.391	0.0		
$52\bar{6}$	1.387	0.0		
$5.1.\overline{10}$	1.387	0.1		
$22\bar{7}$	1.386	0.0		
203	1.384	0.0		
$31\bar{9}$	1.383	0.1		
$23\bar{4}$	1.382	0.0		
006	1.380	0.0		
			1.364	½
			1.345	2
			1.324	2
			1.269	1
			1.245	1
			1.222	2
			1.197	1
			1.088	2

TABLE I—*Continued*

Indices *hkl*	Spacing calculated	Relative intensity calculated	Spacing measured	Relative intensity observed
			1.050	½
			1.020	1
			0.977	½ (broad)
			0.897	1
			0.873	1
			0.822	1

* The intensities were estimated visually on a scale of ten, where ten represents the intensity of the strongest line.

TABLE II

Relative intensities of *x*-ray diffraction spots from a Weissenberg equator photograph of sylvanite taken with the crystal rotating around the *a*-axis.

Indices *hkl*	Spacing calculated	Relative intensity		CuK-radiation†
		observed*	calculated	
001	8.278	0	0.0	$\alpha_1+\alpha_2$
002	4.139	0	0.2	$\alpha_1+\alpha_2$
003	2.759	0	0.0	$\alpha_1+\alpha_2$
004	2.070	s	5.3	$\alpha_1+\alpha_2$
005	1.656	0	0.0	$\alpha_1+\alpha_2$
006	1.380	0	0.0	$\alpha_1+\alpha_2$
007	1.183	0	0.0	$\alpha_1+\alpha_2$
008	1.035	m	0.7	α_1
009	0.920	0	0.0	α_1
0.0.10	0.828	w	0.1	α_1
010	4.480	w	0.4	$\alpha_1+\alpha_2$
020	2.240	s	4.1	$\alpha_1+\alpha_2$
030	1.493	m	0.4	$\alpha_1+\alpha_2$
040	1.120	w	0.2	$\alpha_1+\alpha_2$
050	0.896	m	0.5	α_1
011	3.940	w	0.7	$\alpha_1+\alpha_2$
012	3.040	s	10.0	$\alpha_1+\alpha_2$
013	2.349	w	0.3	$\alpha_1+\alpha_2$
014	1.879	w	0.1	$\alpha_1+\alpha_2$
015	1.553	w	0.1	$\alpha_1+\alpha_2$
016	1.318	m	1.6	$\alpha_1+\alpha_2$
017	1.143	0	0.0	$\alpha_1+\alpha_2$
018	1.008	w	0.1	$\alpha_1+\alpha_2$
019	0.901	0	0.0	α_1
0.1.10	0.814	s	1.2	α_1

TABLE II—*Continued*

Indices *hkl*	Spacing calculated	Relative intensity observed*	Relative intensity calculated	CuK-radiation†
021	2.162	w	0.8	$\alpha_1+\alpha_2$
022	1.970	w	0.3	$\alpha_1+\alpha_2$
023	1.739	w	0.4	$\alpha_1+\alpha_2$
024	1.520	m	1.7	$\alpha_1+\alpha_2$
025	1.331	w	0.2	$\alpha_1+\alpha_2$
026	1.175	w	0.1	$\alpha_1+\alpha_2$
027	1.046	w	0.1	$\alpha_1+\alpha_2$
028	0.939	m	0.5	α_1
029	0.851	0	0.1	α_1
031	1.470	w	0.5	$\alpha_1+\alpha_2$
032	1.405	m	0.6	$\alpha_1+\alpha_2$
033	1.313	w	0.3	$\alpha_1+\alpha_2$
034	1.211	w	0.3	$\alpha_1+\alpha_2$
035	1.109	0	0.2	$\alpha_1+\alpha_2$
036	1.013	w	0.4	$\alpha_1+\alpha_2$
037	0.927	0	0.1	α_1
038	0.850	m	0.2	α_1
039	0.783	w	0.4	α_1
041	1.110	0	0.3	$\alpha_1+\alpha_2$
042	1.081	m	0.3	α_1
043	1.038	0	0.2	α_1
044	0.985	w	0.1	α_1
045	0.928	0	0.2	α_1
046	0.870	m	0.4	α_1
047	0.813	0	0.3	α_1
051	0.891	0	0.1	α_1
052	0.876	0	0.0	α_1
053	0.852	0	0.1	α_1
054	0.822	m	0.8	α_1
055	0.788	0	0.3	α_1

* Denotation of symbols: s, strong; m, medium; w, weak.

† The symbol $\alpha_1+\alpha_2$ denotes an unresolved spot resulting from α_1 and α_2 rays together; the symbol α_1 denotes a spot resulting from α_1 rays alone.

TABLE III

Relative intensities of *x*-ray diffraction spots from a Weissenberg equator photograph of sylvanite taken with the crystal rotating around the *b*-axis.

Indices *hkl*	Spacing calculated	Relative intensity		CuK-radiation
		observed	calculated	
100	5.072	w	1.8	$\alpha_1+\alpha_2$
200	2.536	w	0.2	$\alpha_1+\alpha_2$
300	1.691	s	2.6	$\alpha_1+\alpha_2$
400	1.268	m	1.2	$\alpha_1+\alpha_2$
500	1.014	w	0.0	α_1
600	0.845	w	0.1	α_1
$10\bar{2}$	7.295	w	0.5	$\alpha_1+\alpha_2$
$20\bar{4}$	3.647	w	0.2	$\alpha_1+\alpha_2$
$30\bar{6}$	2.432	0	0.0	$\alpha_1+\alpha_2$
$40\bar{8}$	1.824	s	1.6	$\alpha_1+\alpha_2$
$5.0.\overline{10}$	1.459	w	0.0	$\alpha_1+\alpha_2$
$6.0.\overline{12}$	1.216	m	0.7	$\alpha_1+\alpha_2$
$7.0.\overline{14}$	1.042	w	0.0	α_1
$8.0.\overline{16}$	0.912	w	0.0	α_1
$9.0.\overline{18}$	0.811	w	0.0	α_1
002	4.139	w	0.2	$\alpha_1+\alpha_2$
$10\bar{4}$	2.943	w	0.3	$\alpha_1+\alpha_2$
$20\bar{6}$	2.181	0	0.0	$\alpha_1+\alpha_2$
$30\bar{8}$	1.709	s	3.8	$\alpha_1+\alpha_2$
$4.0.\overline{10}$	1.397	w	0.1	$\alpha_1+\alpha_2$
$5.0.\overline{12}$	1.179	w	0.1	$\alpha_1+\alpha_2$
$6.0.\overline{14}$	1.018	0	0.0	α_1
$7.0.\overline{16}$	0.895	s	0.8	α_1
$8.0.\overline{18}$	0.799	w	0.1	α_1
102	2.386	0	0.0	$\alpha_1+\alpha_2$
004	2.070	s	6.6	$\alpha_1+\alpha_2$
$10\bar{6}$	1.744	w	0.2	$\alpha_1+\alpha_2$
$20\bar{8}$	1.472	0	0.0	$\alpha_1+\alpha_2$
$3.0.\overline{10}$	1.258	0	0.0	$\alpha_1+\alpha_2$
$4.0.\overline{12}$	1.091	w	0.3	$\alpha_1+\alpha_2$
$5.0.\overline{14}$	0.960	0	0.0	α_1
$6.0.\overline{16}$	0.854	s	0.7	α_1
202	1.642	w	0.1	$\alpha_1+\alpha_2$
104	1.526	w	0.4	$\alpha_1+\alpha_2$
006	1.380	w	0.1	$\alpha_1+\alpha_2$
$10\bar{8}$	1.232	0	0.0	$\alpha_1+\alpha_2$
$2.0.\overline{10}$	1.097	0	0.0	α_1
$3.0.\overline{12}$	0.981	s	0.9	α_1
$4.0.\overline{14}$	0.882	w	0.1	α_1
$5.0.\overline{16}$	0.798	w	0.1	α_1
302	1.247	w	0.1	$\alpha_1+\alpha_2$

TABLE III—*Continued*

Indices *hkl*	Spacing calculated	Relative intensity		CuK-radiation
		observed	calculated	
204	1.193	w	0.1	$\alpha_1+\alpha_2$
106	1.118	0	0.0	$\alpha_1+\alpha_2$
008	1.035	m	0.9	α_1
$1.0.\overline{10}$	0.951	w	0.1	α_1
$2.0.\overline{12}$	0.872	0	0.0	α_1
$3.0.\overline{14}$	0.800	0	0.0	α_1
402	1.003	0	0.0	α_1
304	0.998	m	0.5	α_1
206	0.932	w	0.0	α_1
108	0.882	w	0.3	α_1
0.0.10	0.828	w	0.1	α_1
502	0.838	0	0.0	α_1
404	0.821	s	1.2	α_1
306	0.795	m	0.3	α_1
$20\bar{2}$	4.190	w	0.3	$\alpha_1+\alpha_2$
$30\bar{4}$	2.980	m	10.0	$\alpha_1+\alpha_2$
$40\bar{6}$	2.204	0	0.1	$\alpha_1+\alpha_2$
$50\bar{8}$	1.723	w	0.2	$\alpha_1+\alpha_2$
$6.0.\overline{10}$	1.407	0	0.0	$\alpha_1+\alpha_2$
$7.0.\overline{12}$	1.186	m	1.5	$\alpha_1+\alpha_2$
$8.0.\overline{14}$	1.023	w	0.0	α_1
$9.0.\overline{16}$	0.900	w	0.1	α_1
$10.0.\overline{18}$	0.802	w	0.0	α_1
$30\bar{2}$	2.405	w	0.1	$\alpha_1+\alpha_2$
$40\bar{4}$	2.095	m	3.0	$\alpha_1+\alpha_2$
$50\bar{6}$	1.767	w	0.0	$\alpha_1+\alpha_2$
$60\bar{8}$	1.490	w	0.8	$\alpha_1+\alpha_2$
$7.0.\overline{10}$	1.272	w	0.0	$\alpha_1+\alpha_2$
$8.0.\overline{12}$	1.102	0	0.0	$\alpha_1+\alpha_2$
$9.0.\overline{14}$	0.968	0	0.0	α_1
$10.0.\overline{16}$	0.862	s	1.4	α_1
$40\bar{2}$	1.652	0	0.0	$\alpha_1+\alpha_2$
$50\bar{4}$	1.542	w	0.1	$\alpha_1+\alpha_2$
$60\bar{6}$	1.397	w	0.1	$\alpha_1+\alpha_2$
$70\bar{8}$	1.248	m	1.8	$\alpha_1+\alpha_2$
$8.0.\overline{10}$	1.112	0	0.0	$\alpha_1+\alpha_2$
$9.0.\overline{12}$	0.993	w	0.0	α_1
$10.0.\overline{14}$	0.892	0	0.0	α_1
$11.0.\overline{16}$	0.807	w	0.2	α_1
$50\bar{2}$	1.252	w	0.0	$\alpha_1+\alpha_2$
$60\bar{4}$	1.203	w	0.3	$\alpha_1+\alpha_2$
$70\bar{6}$	1.130	0	0.0	$\alpha_1+\alpha_2$
$80\bar{8}$	1.048	0	0.0	α_1
$9.0.\overline{10}$	0.963	w	0.0	α_1

TABLE III—*Continued*

Indices *hkl*	Spacing calculated	Relative intensity		CuK-radiation
		observed	calculated	
$10.0.\overline{12}$	0.883	s	1.3	α_1
$11.0.\overline{14}$	0.810	w	0.0	α_1
$60\bar{2}$	1.007	w	0.1	α_1
$70\bar{4}$	0.981	s	1.0	α_1
$80\bar{6}$	0.941	0	0.0	α_1
$90\bar{8}$	0.892	0	0.0	α_1
$10.0.\overline{10}$	0.838	w	0.0	α_1
$70\bar{2}$	0.841	0	0.0	α_1
$80\bar{4}$	0.826	0	0.0	α_1
$90\bar{6}$	0.802	w	0.1	α_1

TABLE IV

Relative intensities of x-ray diffraction spots from a Weissenberg equator photograph taken with the crystal rotating around the [201] zone-axis.

Indices *hkl*	Spacing calculated	Relative intensity		CuK-radiation
		observed	calculated	
010	4.480	w	0.9	$\alpha_1+\alpha_2$
020	2.240	s	9.9	$\alpha_1+\alpha_2$
030	1.493	m	1.1	$\alpha_1+\alpha_2$
040	1.120	w	0.3	α_1
050	0.896	w	1.2	α_1
$10\bar{2}$	7.295	w	1.0	$\alpha_1+\alpha_2$
$20\bar{4}$	3.647	w	0.4	$\alpha_1+\alpha_2$
$30\bar{6}$	2.432	0	0.1	$\alpha_1+\alpha_2$
$40\bar{8}$	1.824	s	3.1	$\alpha_1+\alpha_2$
$5.0.\overline{10}$	1.459	0	0.1	$\alpha_1+\alpha_2$
$6.0.\overline{12}$	1.216	m	0.9	α_1
$7.0.\overline{14}$	1.042	w	0.1	α_1
$8.0.\overline{16}$	0.912	0	0.0	α_1
$9.0.\overline{18}$	0.811	0	0.0	α_1
$11\bar{2}$	3.818	w	1.4	$\alpha_1+\alpha_2$
$21\bar{4}$	2.828	0	0.1	$\alpha_1+\alpha_2$
$31\bar{6}$	2.137	s	10.0	$\alpha_1+\alpha_2$
$41\bar{8}$	1.689	w	0.3	$\alpha_1+\alpha_2$
$5.1.\overline{10}$	1.387	w	0.2	$\alpha_1+\alpha_2$
$6.1.\overline{12}$	1.173	0	0.0	α_1
$7.1.\overline{14}$	1.015	m	1.4	α_1
$8.1.\overline{16}$	0.893	0	0.1	α_1
$9.1.\overline{18}$	0.798	w	0.3	α_1
$12\bar{2}$	2.141	0	0.2	$\alpha_1+\alpha_2$

TABLE IV—*Continued*

Indices *hkl*	Spacing calculated	Relative intensity		CuK-radiation
		observed	calculated	
$22\bar{4}$	1.909	0	0.0	$\alpha_1+\alpha_2$
$32\bar{6}$	1.648	w	0.4	$\alpha_1+\alpha_2$
$42\bar{8}$	1.414	w	1.3	$\alpha_1+\alpha_2$
$5.2.\overline{10}$	1.222	0	0.0	$\alpha_1+\alpha_2$
$6.2.\overline{12}$	1.069	w	0.8	α_1
$7.2.\overline{14}$	0.945	w	0.2	α_1
$8.2.\overline{16}$	0.845	0	0.0	α_1
$13\bar{2}$	1.463	w	0.2	$\alpha_1+\alpha_2$
$23\bar{4}$	1.382	w	0.0	$\alpha_1+\alpha_2$
$33\bar{6}$	1.272	w	1.2	$\alpha_1+\alpha_2$
$43\bar{8}$	1.155	w	0.3	$\alpha_1+\alpha_2$
$5.3.\overline{10}$	1.044	w	0.0	α_1
$6.3.\overline{12}$	0.943	w	0.1	α_1
$7.3.\overline{14}$	0.855	w	0.9	α_1
$8.3.\overline{16}$	0.778	0	0.0	α_1
$14\bar{2}$	1.107	0	0.1	α_1
$24\bar{4}$	1.071	w	0.0	α_1
$34\bar{6}$	1.017	w	0.5	α_1
$44\bar{8}$	0.954	w	0.2	α_1
$5.4.\overline{10}$	0.888	w	0.0	α_1
$6.4.\overline{12}$	0.824	w	0.2	α_1
$15\bar{2}$	0.889	w	0.1	α_1
$25\bar{4}$	0.870	w	0.0	α_1
$35\bar{6}$	0.841	w	0.1	α_1
$45\bar{8}$	0.804	w	0.8	α_1

where 2θ denotes the angle between the incident and diffracted beams, F the structure factor, and j the number of cooperating planes. On the powder photograph the α_1 and α_2 lines were not resolved. Tables II, III, and IV contain the observed and calculated intensities of diffraction spots in three Weissenberg equator photographs taken with copper K-radiation with the crystals rotating around the a-, b-, and [201] zone-axes, respectively. The intensities I_W of the α_1 spots (where the α_1 and α_2 spots were resolved) on the Weissenberg equator films were calculated from the formula

$$I_W = \frac{1 + \cos^2 2\theta}{\sin 2\theta} \mid F \mid^2,$$

and the intensities I_W of the unresolved α_1 and α_2 spots on the same films from the formula

$$I_W = 1.5 \frac{1 + \cos^2 2\theta}{\sin 2\theta} \mid F \mid^2.$$

The atomic *f*-values of James and Brindley[20] were used except that in view of the replacement of part of the silver atoms by gold atoms, in place of the *f*-value of silver a composite value was used made up of 93 per cent of the *f*-value of silver and 7 per cent of the *f*-value of gold. No correction was made for absorption. However, small crystals were found elongated parallel to two of the rotation axes, namely, the *a*-axis and [201] zone-axis, with cross sections perpendicular to the rotation axes of almost equal diameters in all directions, and it is believed that in these cases any error due to the influence of crystal shape is small. The intensities used are relative and were estimated visually. For computation of a Fourier series leading to the construction of the projection of the structure on the plane 010, the intensities on the Weissenberg equator photograph taken with the crystal rotating around the *b*-axis were used, and these were obtained by visual comparison of the diffraction spots on the film with a standard scale of spots prepared in the Department of Chemistry of the Johns Hopkins University.[21] On this standard scale the intensities are taken to be proportional to the exposure times of the spots to a beam of constant energy output. The observed intensities obtained by comparison with the standard scale were multiplied by 2/3 for the spots in which the $\alpha_1\alpha_2$-doublet is not resolved to reduce them to the same basis as the spots due to α_1-radiation alone. The resulting values divided by the Lorentz and polarization factors yielded numbers proportional to the squares of the absolute values of the structure factors. The square roots of these numbers were extracted and positive and negative signs were affixed in accordance with those of the F's obtained from the structure arrived at by comparison of observed and calculated intensities. The experimental F-values are listed in Table V, along with the calculated F-values, which are given for comparison. The synthesis of the two-dimensional Fourier series was carried out by the method devised by Patterson[22] and improved by Patterson and Tunell.[23] The values of $A(x, y) = \rho(x, y) + K$, where $\rho(x, y)$ denotes the projected electron density and K denotes a constant, were computed at 1800 points in the half projection, corresponding to division of each of the unit cell edges into 60 parts. Vertical sections were drawn along the lines of the grid work parallel to the *a*-axis, and from them a contour map of $A(x, y)$ was plotted (Fig. 3). The positions of the atoms found from the contour map are as given at the beginning of this section. The largest peaks shown on the contour map are at $x=0$, $z=0$ and $x=0$, $z=\frac{1}{2}$, where the gold

---

[20] *Zeits. Krist.*, **78,** 475 (1931).

[21] The writer is indebted to Dr. David Harker for the use of this scale.

[22] *Phil. Mag.*, (7), **22,** 753–754 (1936).

[23] Forthcoming article in *Am. Mineral.*

Table V

F-values of sylvanite for *hol* planes. The upper values, obtained from an equator Weissenberg photograph,* are those used in the calculation of the Fourier projection. The lower values, given for comparison, are those calculated from the atomic positions scaled from the contour map.

l \ *h*	$\bar{11}$	$\bar{10}$	$\bar{9}$	$\bar{8}$	$\bar{7}$	$\bar{6}$	$\bar{5}$	$\bar{4}$	$\bar{3}$	$\bar{2}$	$\bar{1}$	0	1	2	3	4	5	6
18		+ 7 + 7.2	− 6 − 1.9	+11 +12.4														
16	+16 +20.0	+99 +68.2	+13 +14.2	− 9 − 7.8	+62 +56.8	+59 +49.0	− 8 − 9.1											
14	+ 7 + 4.8	0 + 7.6	0 + 5.4	+10 +11.4	+12 +13.5	0 − 1.9	0 + 4.9	+22 +22.6	0 + 3.0									
12		+105 + 68.0	+10 + 7.6	0 − 4.6	+42 +73.1	+42 +50.5	−12 −15.6	+22 +35.6	+71 +68.1	0 + 6.2								
10		+ 7 + 9.7	+10 +12.2	0 + 6.7	+ 8 + 9.3	0 + 5.8	+ 7 + 9.3	+15 +19.7	0 + 3.7	0 − 3.2	+18 +20.4	+13 +14.5						
8			0 + 1.6	0 + 1.7	+41 +79.4	+18 +47.1	−10 −21.7	+45 +56.7	+81 +90.4	0 − 1.2	0 + 6.0	+52 +70.6	+22 +31.7					
6			+15 +15.3	0 − 0.5	0 + 5.9	+ 8 +15.2	+ 6 + 9.9	0 +11.9	0 + 7.9	0 + 4.5	+10 +20.9	+ 8 +13.1	0 − 6.8	+11 +11.1	+22 +22.5			
4				0 + 8.2	+71 +70.9	+21 +31.6	−14 −19.5	+29 +70.5	+ 19 +102.5	− 6 −13.1	+ 5 +18.5	+ 41 +105.0	+14 +33.3	−10 −13.4	+44 +50.6	+63 +52.7		
2					0 + 5.1	+20 +20.5	+ 8 + 5.7	0 + 2.1	+ 7 +15.6	+ 4 +13.4	+ 4 +14.4	+ 4 +12.5	0 + 0.9	+ 8 +14.7	+12 +20.1	0 − 3.2	0 + 0.1	
0						+19 +20.7	−12 −10.7	+41 +62.8	+82 +75.9	−10 −17.6	+ 9 +31.7		+ 9 +31.7	−10 −17.6	+82 +75.9	+41 +62.8	−12 −10.7	+19 +20.7

---

* The observed values of the intensities of $\bar{3}04$ and 004 are too low on this Weissenberg film apparently owing to an effect of the crystal shape; the observed intensities of $\bar{3}04$ and 004 on the powder photograph (cf. Table I) are in agreement with those calculated.

atoms were placed by the trial and error method; the second largest peaks are at $x=0.298$, $z=0.999$ and $x=0.277$, $z=0.235$, very close to the points at which the tellurium atoms were placed by the trial and error method; the third largest peaks are at $x=0$, $z=\frac{1}{4}$ and $x=0$, $z=\frac{3}{4}$, where the silver

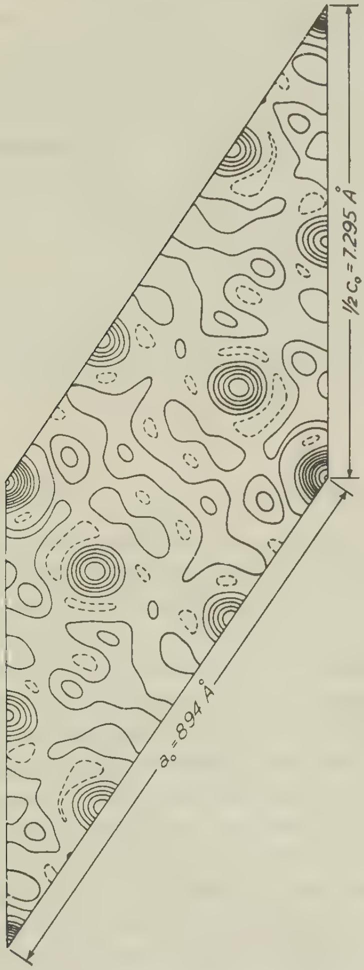

FIG. 3. Fourier projection along the symmetry axis (b-axis) of the structure of sylvanite. The contour map within the parallelogram represents the projection of one half of the unit cell. The peaks at the corners of the parallelogram represent gold atoms. The peaks midway between the corners along the vertical boundaries represent silver atoms. The peaks along the inclined boundaries and within the parallelogram represent tellurium atoms. Dotted lines are depression contours.

atoms were placed by the trial and error method. There are no other large peaks in the projection. After the contour map was drawn the intensities were recalculated from the positions of the atoms found by means of the contour map. The agreement of observed and calculated intensities is best in the case of the powder spectrum (Table I), as would be expected. The agreement of the observed and calculated intensities of the Weissenberg equator photographs (Tables II, III, and IV) is also fairly good, especially in view of the highly absorbing nature of the material. Moreover, the Fourier series calculated from the intensities of the diffraction spots on the Weissenberg equator photograph taken with the crystal rotating about the *b*-axis yielded atomic positions not differing more than 1/100 of the unit cell edge in any coordinate from those previously determined by comparison of observed and calculated intensities of the powder spectrum and the Weissenberg equator photographs taken with the crystals rotating around the *a*-axis and the [201] zone-axis. Hence the values of the parameters are believed to be correct within a tolerance of ±0.01.

Discussion of the Atomic Arrangement

In the sylvanite structure each gold atom and each silver atom is surrounded octahedrally by six tellurium atoms and each tellurium atom is surrounded octahedrally by three tellurium atoms, two gold atoms, and one silver atom, or by three tellurium atoms, two silver atoms, and one gold atom. The orientation of the octahedra is most easily seen from Fig. 1,C. Two neighbors of each gold atom have their centers situated nearly on a line through the center of the gold atom parallel to the *a*-axis; the other four neighbors have their centers not far from a plane through the center of the gold atom perpendicular to the *a*-axis. Two neighbors of each silver atom likewise have their centers situated nearly on a line through the center of the silver atom parallel to the *a*-axis and the other four neighbors have their centers not far from a plane through the center of the silver atom perpendicular to the *a*-axis. Two neighbors of each tellurium atom also have their centers situated nearly on a line through the center of the tellurium atom parallel to the *a*-axis and the other four neighbors have their centers not far from a plane through the center of the tellurium atom perpendicular to the *a*-axis. The distances between the gold and tellurium atoms are 2.67 Å, 2.76 Å, and 3.26 Å. The distances between the silver and tellurium atoms are 2.69 Å, 2.94 Å, and 3.19 Å. The distances between tellurium atoms are 2.88 Å, 3.56 Å, 3.64 Å,[24] and 3.64 Å. All these distances are shown in Fig. 1,C. The structure can be described as consisting of lines of atoms parallel to the a-axis. These lines are at $y=0$, $z=0$, at $y=0.433$, $z=\frac{1}{4}$, at $y=0$, $z=\frac{1}{2}$, and at $y=0.567$, $z=\frac{3}{4}$. Along these lines metal atoms are separated by pairs of tellurium atoms, the metal atoms lying exactly on the lines and the tellurium atoms lying close to them. The metal atoms also lie in planes parallel to the b- and c-axes at $x=0$ with two layers of tellurium atoms separating the metal atoms.

---

[24] The two distances 3.64 Å are not required by symmetry to be the same.

VERMICULITE AND HYDROBIOTITE

ROBERT F. RUTHRUFF,[1]
Chempats Incorporated, Wilmington, Delaware.

ABSTRACT

An analysis of hydrobiotite tends to confirm the findings of Gruner[2] that this mineral consists of interstratified layers of vermiculite and biotite. The indications are that the layers of the two minerals are present in a 1:1 ratio although by using somewhat less reasonable assumptions a ratio of 3 vermiculite :2 biotite is obtained.

On heating with dilute sulfuric acid all oxides, with the exception of silica, are removed from vermiculite, the final silica being obtained in the form of white plates. The complete removal of oxides other than silica from hydrobiotite by similar treatment is much more difficult. Hydrobiotite saturated with concentrated sulfuric acid and then exposed to air over a considerable period, or steamed for a shorter time, exfoliates greatly, a behavior not shown by vermiculite.

While the vermiculites have long been recognized as complex minerals of rather indefinite composition (the sixth edition of *Dana* lists no less than 14 varieties), Gruner[2] was the first to distinguish clearly between true vermiculite,

$$(OH)_2(Mg, Fe)_3(Si, Al)_4O_{10}\cdot 4H_2O$$

and hydrobiotite which consists of interstratified layers of true vermiculite and biotite,

$$(OH)_2K(Mg, Fe)_3(Si, Al)_4O_{10}\cdot 4H_2O.$$

Vermiculite and hydrobiotite differ markedly in several respects. Since the present major source of supply (Libby, Montana) of minerals of this type furnishes hydrobiotite and as the differences between vermiculite and hydrobiotite have not been generally recognized,[3] the following observations with respect to these two minerals may be of interest.

A large sample of hydrobiotite (Libby, Montana) was successively quartered and then analyzed, the results being shown in Table 1. For comparison, the average of seven vermiculite analyses collected by Gruner[2] is also shown (Column 2). If it is assumed that structurally a calcium ion is equivalent to an alkali metal ion in hydrobiotite, then the atom distribution is approximately as follows:

---

[1] Present address, 1711 West 100th Street, Chicago, Illinois.

[2] Gruner, *Am. Mineral.*, **19**, 557–575 (1935).

[3] For example, Hansen, Samuel and Forni, Sorption of water vapor by vermiculite and its silica: *Ind. Eng. Chem.*, **32**, 116–118 (1940). In this work hydrobiotite was investigated although the vermiculite composition and structural formula was used throughout.

Silicon	11.2	17.05	27.90
Aluminum	5.85		
Iron	1.45	10.85	
Magnesium	9.4		
Potassium plus Calcium	2.0		

The above, after rounding off and transferring one atom of aluminum from tetrahedral to octahedral coordination becomes:

TABLE 1. ANALYSES OF VERMICULITES AND HYDROBIOTITES

Column	1	2	3	4
SiO_2	43.3	46.0	42.3	43.5
Al_2O_3	19.0	17.7	19.5	18.4
Fe_2O_3	7.4	5.5	7.7	8.2
MgO	24.0	30.8	24.5	25.0
CaO	1.6		6.0	
K_2O	4.7			4.9
Total	100.0	100.0	100.0	100.0
Loss on ignition	11.0	20.1	12.1	10.8

1. Analysis of hydrobiotite. (True total, 99.15%, corrected to 100%.)
2. Average of seven vermiculite analyses collected by Gruner,[2] reduced to water free basis.
3. Calculated analysis of hydrobiotite assuming vermiculite and biotite sheets in 1:1 ratio.
4. Calculated analysis of hydrobiotite assuming vermiculite and biotite sheets in 3:2 ratio.

Silicon	11.0	16
Aluminum	5.0	
Iron	1.5	12
Magnesium	9.5	
Aluminum	1.0	

which reduces to

$$\left.\begin{array}{l}(OH)_2K(Mg_{2.25}Fe_{0.75})(Si_{2.75}Al_{1.25})O_{10} \\ (OH)_2(Al_{0.5}Mg_{2.50})(Si_{2.75}Al_{1.25})O_{10}\end{array}\right\}4H_2O$$

equivalent to alternating layers of vermiculite and biotite. The calculated analysis of this complex is given in Column 3, Table 1.

While isomorphic substitution of a calcium ion for an alkali metal ion, particularly a sodium ion is extremely common, it is possible for a calcium ion to occur in octahedral coordination. If it is assumed that a calcium ion is structurally equivalent to magnesium in hydrobiotite, then the atom distribution is approximately as follows:

Silicon	14.4	21.9	36.25
Aluminum	7.5		
Iron	1.85	14.35	
Mg+Ca	12.5		
Potassium	2.0		

Again rounding off these values and transferring 1.5 aluminum atoms from tetrahedral to octahedral positions there results:

Silicon	14.0	20
Aluminum	6.0	
Iron	1.5	15
Aluminum	1.5	
Magnesium	12.0	

which reduces to:

$$\left.\begin{array}{l} (OH)_2(Al_{0.50}Mg_{2.50})(Al_{1.2}Si_{2.8})O_{10} \\ (OH)_2K(Fe_{0.75}Mg_{2.25})(Al_{1.2}Si_{2.8})O_{10} \\ (OH)_2(Al_{0.50}Mg_{2.50})(Al_{1.2}Si_{2.8})O_{10} \\ (OH)_2K(Fe_{0.75}Mg_{2.25})(Al_{1.2}Si_{2.8})O_{10} \\ (OH)_2(Al_{0.50}Mg_{2.50})(Al_{1.2}Si_{2.8})O_{10} \end{array}\right\} 8H_2O$$

Here the configuration of biotite and vermiculite layers is *VBVBV*. The calculated analysis of this complex is given in Column 4 of Table 1. For reasons already given, it is believed that the structure represented by biotite and vermiculite layers in 1:1 ratio is the more likely of the two alternatives.

When hydrobiotite is treated with hot dilute sulfuric acid more or less pure silica lamellae (lamisilite) result.[3,4] In a study of the suitability of silica lamellae from both vermiculite and hydrobiotite as substrates for catalysts, the behavior of these two minerals when treated with acids was examined intensively. Data obtained during the treatment of true vermiculite from the Georgia-Carolinas mineral district are presented in Table 2.

In the first pair of experiments of Table 2, the mineral (through 4 mesh) was refluxed for 3 hours with a 1:2 mixture (by weight) of sulfuric acid and water, 1.1 parts by weight of acid being used per 1.0 part by weight of mineral. This amount of acid is that theoretically required to remove all oxides (except silica) as the normal sulfates. After the reaction was ended the product was thoroughly washed and dried at 110°C. About 43g. of quite pure silica was obtained. It has been stated[5] that hydrogen peroxide exfoliates vermiculite in the cold. Groves[6] found that other oxidizing agents act similarly, but not as energetically. For certain reasons

[4] Guthrie and Wilbor, U. S. Patent 1,898,774. February 21, 1933.

[5] Gruner, *Am. Mineral.*, **24,** 428–433 (1934).

[6] Groves, *Nature*, **144,** 554 (1939).

TABLE 2. ACID TREATMENT OF VERMICULITE

Exp. No.	Verm. g.	H_2SO_4 g.	H_2O g.	CrO_3 g.	Time hrs.	Dry Wt. g.
1	100	110	220	—	3	43.4
2	100	110	220	—	3	42.9
3	100	110	220	10	3	42.4
4	100	275	550	—	3	45.0
5	100	234	468	—	3	39.4

Experiment 1. On exposure to air, weight increases to 50.35g. (16% increase).

Experiment 2. Apparent density of the product, 0.477.

Experiment 3. Apparent density of product 0.471. Product colored with chromate ion even after thorough washing.

Experiment 4. Partially exfoliated material employed. 100g. exfoliated charge equivalent to 117.7g. raw mineral. 45.0g. product from 100g. exfoliated = 117.7g. raw mineral equivalent to 38.2g. product from 100g. raw mineral. Also, proportions are equivalent to 100g. raw mineral : 234g. acid : 468g. water. Compare with Experiment 5.

Experiment 5. Compare with Experiments 1 and 2.

the action of chromium trioxide was of interest. Accordingly, 100g. of vermiculite was soaked in a solution containing 10g. of this strong oxidizing agent in 220g. of water. No reaction was observed over a period of several days so the usual amount of acid was added and the mixture was refluxed for 3 hours. The product weighed 42.4g. (Experiment 3, Table 2). The use of chromium trioxide gave rise to no exfoliation and had little if any effect on the progress of the leaching reaction.

In Experiment 4 (Table 2) partially exfoliated vermiculite was leached. Due to the large bulk of the exfoliated charge, a much larger volume of the acid-water mixture than usual was required but the acid concentration was kept constant. The product weighed 45.0g., equivalent to 38.2g. per 100g. of raw (unexfoliated) mineral. To determine whether the more complete cleanup resulted from the use of exfoliated mineral, or from the large excess acid employed, Experiment 5 was run in which raw mineral was refluxed with the usual 1:2 acid-water mixture in an amount equivalent to that employed in Experiment 4. The product weighed 39.4g. indicating that exfoliation has little if any effect on the leaching process but that a large excess of acid gives an appreciably better cleanup. A large number of experiments that need not be considered in detail indicated that very pure silica lamellae are obtained using 1.0 raw vermiculite, 2.2 acid and 2.5 water (all parts by weight) and refluxing for three hours.

It is interesting to note that vermiculite when soaked in concentrated sulfuric acid (1g. mineral per 1.1g. acid) and then exposed to air effloresces greatly with the elimination of salts, but undergoes no additional change. This is in striking contrast to the behavior of hydrobiotite when treated similarly (see below).

The silica lamellae obtained from vermiculite by acid leaching are themselves of high purity but are mixed with a small amount of granular, heavy greenish material which is easily separated from a suspension of the silica plates by settling. The thus purified silica formed an excellent catalyst substrate.

A somewhat similar series of experiments was run with hydrobiotite, the results being presented in Table 3. When refluxed with the 1:2 (by weight) sulfuric acid-water mixture, using 1g. mineral per 1.1g. sulfuric acid, the final product weighed 60g., the cleanup being much less complete than with vermiculite (Experiment 1). The product from hydrobiotite consists of lamellae of silica mixed with a considerable amount of darker colored plates. Hydrobiotite exfoliates markedly when boiled with the diluted acid giving a final product weighing about 0.25g. per cc. which however undergoes additional exfoliation on heating. True vermiculite does not visibly exfoliate during refluxing and the resulting product does not exfoliate on heating. Hydrobiotite does not exfoliate in a cold solution of chromium trioxide, and when acid is added and the mixture is refluxed, removal of oxides other than silica is little better than in the absence of the oxidizing agent as Experiment 2 shows.

TABLE 3. ACID TREATMENT OF HYDROBIOTITE

Exp. No.	Hydro-biotite	H_2SO_4	H_2O	CrO_3	Time	Dry Wt.
	g.	g.	g.	g.	hrs.	g.
1	100	110	220	—	3	60.0
2	100	110	220	10	3	58.1
3	100	275	550	—	3	56.0
4	100	110	220	—	6	51.4
5	100	110	440	—	6	64.1
6	100	110	440	—	6	53.6
7	100	110	220	—	5	50.6

Experiment 1. Apparent density of product 0.261.

Experiment 2. Apparent density of product 0.264. Final product colored with chromate ion.

Experiment 3. Compare with Experiment 1.

Experiment 4. Compare with Experiments 1 and 3. Weight of product after exposure to air, 57.2g. (11% increase).

Experiment 5. Soaked in the concentrated acid 48 hours, exposed to air 72 hours. Volume increase tenfold. Weight after exposure to air, 238g. 238g. − 210g. = 28g. water absorbed from air. 440g. − 28g. = 412g. water added before refluxing.

Experiment 6. Compare with Experiments 4 and 5.

Experiment 7. Soaked in concentrated acid 24 hours, steamed 1 hour, then sufficient water added to give 430g. total before refluxing for five hours.

While vermiculite theoretically requires about 1.1g. acid per gram to unite with all oxides, except silica, to form normal sulfates, hydrobiotite requires in the neighborhood of 1.2g. per gram. Accordingly, in Experiment 3, a large excess of acid, 2.75g. per gram of hydrobiotite, was employed and while an improvement is noticeable it is not commensurate with the large additional amount of acid used. On the other hand, on returning to the standard 1.1g. acid per gram of mineral but increasing the treating time from three to six hours a marked improvement in the leaching process followed as Experiment 4 testifies.

Hydrobiotite, when soaked in concentrated sulfuric acid and then exposed to air behaves in a most striking manner. After soaking 100g. hydrobiotite in 110g. concentrated sulfuric acid for 48 hours, the resulting mixture is exposed to air in a thin layer which is turned occasionally. After 24 hours' exposure exfoliation is noticeable and at the end of 2 to 3 days, depending upon humidity conditions, it is complete, the volume increase being as much as ten fold. During exposure to air the mineral gradually becomes white due to the separation of salts. Many investigators[7] have stated or implied that the exfoliation of vermiculite is due to the expulsion of water on heating. Obviously, this is not necessarily true for otherwise exfoliation would be an exceedingly common phenomenon. Groves[6] pointed out that the cold exfoliation of vermiculite in hydrogen peroxide made this theory untenable and the exfoliation of acid soaked hydrobiotite when exposed to air is another case in point. In the present instance, the exfoliation is attributed to the forcing apart of lamellae by sulfate crystals formed between them. When a cork of heat exfoliated vermiculite or hydrobiotite is pinched between the fingers it easily compresses to approximately the original size of the mineral particle from which it was obtained, and the resulting compressed mass forms a coherent whole. Acid exfoliated hydrobiotite, on the other hand, resists compression to a small but noticeable degree, and after compression the resulting material tends to disintegrate into a number of lamellae. During compression of such material the destruction of the sulfate crystals is felt distinctly. Even if this explanation of acid exfoliation of hydrobiotite is correct the question as to the mechanism of thermal exfoliation remains.

Some hydrobiotite, exfoliated with acid as above described, was treated with water and then refluxed (Experiment 5). Because of the exfoliation, twice the normal amount of water was required to give a fluid reaction mixture. The cleanup was very poor, the final product containing considerable insoluble basic aluminum sulfate. To determine if the unusually dilute acid employed was responsible for the formation of this insoluble basic salt, Experiment 6 was run similar to Experiment 4 in all respects with exception of the concentration of the acid employed. The cleanup was almost normal.

---

[7] For example, Crouse, *Eng. Mining Jour.*, **128,** 923 (1929).
Kriegel, *Bull. Am. Ceram. Soc.*, **19,** 94–97 (1940).
Pardie and Larson, *U. S. Geol. Sur. Bull.*, **805B** (1928).

When raw hydrobiotite is steamed for one hour there is no change in the appearance or apparent volume of the mineral. On the other hand, if acid soaked hydrobiotite is steamed for one hour considerable exfoliation occurs. The resulting product, when treated with the standard amount of water and refluxed gives the expected amount of cleanup.

While it is comparatively easy to obtain a pure silica from vermiculite by an acid leach, this was impossible when using raw hydrobiotite. The product from the latter mineral was invariably contaminated with dark flakes believed to be biotite.

ACKNOWLEDGMENT

The author wishes to acknowledge the invaluable aid rendered by Mr. D. Rein during the progress of this work.

OPTIC PROPERTIES OF CORDIERITE IN RELATION TO ALKALIES IN THE CORDIERITE-BERYL STRUCTURE

ROBERT E. FOLINSBEE,
University of Minnesota, Minneapolis, Minnesota.

ABSTRACT

The writer presents a chemical analysis of optically positive, gem quality cordierite from a new occurrence, north of Great Slave Lake. Anomalies in the Shibata (Winchell) variation diagrams, which relate the optic properties of cordierite to the iron-magnesium ratio are noted. The relation of the cordierite structure to that of beryl is clarified, and alkali ion positions in the beryl structure postulated. Alkalies have a pronounced effect on the optic properties of beryl, suggesting, by analogy, that anomalous variations in the optic properties of cordierite are due to variable alkali content. The suggestion is confirmed by graphical presentations of the optic properties of analyzed cordierites.

INTRODUCTION

Eight occurrences of optically positive cordierite are reported in the literature (4, 5, 10, 11, 13, 15, 16, 20). No such cordierite has been synthesized and at the time of Shibata's research (17), relating the optic sign to ferrous iron content, data regarding this optically anomalous group of cordierites were not available.

Cordierite from a new locality, analyzed by the writer (Table 1), is optically positive. This transparent gem-quality cordierite occurs north of Great Slave Lake in an injection and assimilation gneiss of the Scottish highlands type (14). The associated minerals are: garnet, sillimanite, green spinel, graphite, biotite, orthoclase, microcline and oligoclase feldspar, quartz and tourmaline. Single prismatic crystals of the cordierite attain a size of 4 by 2 by 2 inches. These crystals are fractured but yield many fragments of gem size and quality.

If the analysis of this cordierite and three other analyses of optically positive cordierite, for which there are reasonably complete chemical, optical and physical data, are plotted on the Shibata (Winchell) variation diagram (21), the following points are noteworthy (Fig. 1):

(1) Optically positive cordierites vary widely in ferrous iron content (from 15.7 to 44.0 per cent of the $Fe_2Al_4Si_5O_{18}$ molecule).

(2) These cordierites with optic angles greater than 90° occur over the range of iron content over which Winchell postulates both a maximum (83°) and minimum (43°) point on the 2V curve.

(3) The three indices of refraction of all optically positive cordierites are lower than the respective indices of optically negative cordierites of the same Fe/Mg ratio.

(4) The birefringence of optically positive cordierite is greater than that of optically negative cordierite of similar Fe/Mg ratio.

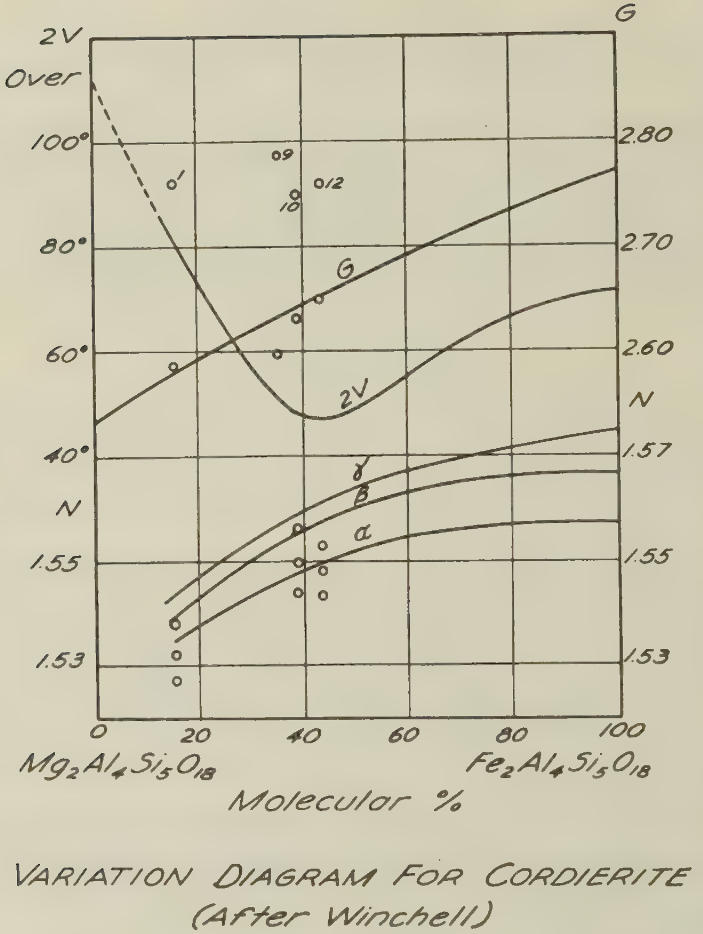

FIG. 1. Optically positive cordierites (Table 4) plotted on the Shibata-Winchell variation diagram. The curves are Winchell's (21), the data from which the curves were derived are omitted.

TABLE 1. CHEMICAL ANALYSIS OF CORDIERITE FROM THE GREAT SLAVE LAKE AREA

	Weight Per cent	Molecular Proportions
SiO_2	48.19	802
Al_2O_3	33.45	328
Fe_2O_3	0.55	3
FeO	8.40	117
MgO	7.95	197
CaO	0.17	3
Na_2O	0.22	3
K_2O	0.02	0
H_2O+	0.67	37
H_2O-	0.01	0
TiO_2	0.01	0
Li_2O	Trace	0
MnO	0.18	3
	99.82	

Analyst—R. E. Folinsbee

MOLECULAR COMPOSITION USING WINCHELL'S FORMULA (21)

	RO	Al_2O_3	SiO_2
MgO	98.5	197	492.5
FeO	58.5	117	292.5
MnO	1.5	3	7.5
Fe_2O_3	3.0	6	15.0
Calculated	161.5	323	807.5
Actual	161.5	328	802

61.0% $Mg_2Al_4Si_5O_{18}$
39.0% $(Fe, Mn)_2Al_4Si_5O_{18}$

It is clear that Winchell, following Shibata, in basing a variation diagram on the Fe/Mg ratio of cordierite, was forced to cull anomalous determinations. To quote Winchell (21):

> The lack of correlation between chemical composition and optic properties is illustrated by the fact that there are almost as many (seven) samples of cordierite which have been analyzed and measured optically that cannot be used in the diagram as the number (eight) used in preparing it. . . . But it seems that some other factor (besides Fe + Mn) has a considerable influence on the optic angle.

The writer will endeavor to account for the variable optic angle and sign of cordierite on the basis of a hitherto undiscussed chemical constituent the alkali content. The problem is approached first by an analogy based on structural relationships, then by inductive reasoning based on experimental evidence.

STRUCTURAL RELATIONSHIP OF CORDIERITE AND BERYL

The pseudo-hexagonal orthorhombic mineral cordierite is closely related to the hexagonal mineral beryl in atomic structure. The existence of this relationship, suggested by Gossner and Mussgnug (8, 9) on the basis of *x*-ray studies, is confirmed by the similarities in the chemical, crystallographic, optical, and physical properties of these two minerals.

The structural formulas are similar, though the relation involves the acceptance of an unusual type of substitution.

Beryl	Be_3	$Al_2\ Si_6$	O_{18}
Cordierite	Mg_2Al	$Al_2\ Si_5Al$	O_{18}

Translating freely from Gossner and Mussgnug (8, 9):

> It is well known that the simple substitution of 2Be = 2Mg would ordinarily involve an essential change in the structure, since the ionic radius of beryllium is .34 Å while that of magnesium is .78 Å. However, for the two silicates cordierite and beryl, we have a special case where the ions Be and Mg, as constituents of a larger space group, can replace each other with no essential change in the structure.

The unit cell dimensions as given by Gossner (8) are comparable:

Cordierite		*Beryl*	
Axis			*Axis*
$a'=b$	17.10 Å	16.0 Å	$(=a\sqrt{3})$
$b'=a$	9.78 Å	9.21 Å	$(=a)$
c	9.33 Å	9.17 Å	$(=c)$

Analogies in the chemical composition of the two minerals, as observed by the writer, are even more pronounced. In cordierite the H_2O+ content ranges from .50 to 3.72%, with the average of 1.50% H_2O+; in beryl it ranges from .37 to 3.00 with the average of 1.5%. The amount of water (or of OH ions) seems to have only a slight effect (19) on the density or optical properties, and to date its structural position has been ignored. It is the writer's opinion that the amount of water in these two minerals is an expression of the degree of alteration of the sample, and that the H_2O+ content forms a good basis for judging the purity and freedom from alteration of an analyzed sample (7, 12, 19).

The H_2O+ content of the Great Slave Lake cordierite is very low (0.67%). There is only one out of fifty analyses reported in the literature in which the water content was lower (7). This was also a gem cordierite (from Ceylon). Special care was taken by the writer in selecting the sample for analysis. A gem fragment was crushed, then hand picked. The fragments were checked under the microscope in oil of index 1.55 in order to ensure freedom from pinite (chlorite), and other alteration products or inclusions. An H_2O+ determination made on the reject proved to be appreciably higher (0.95% H_2O+) than that of the analyzed portion (0.67% H_2O+), though to the unassisted eye the fragments appeared to be of comparable purity.

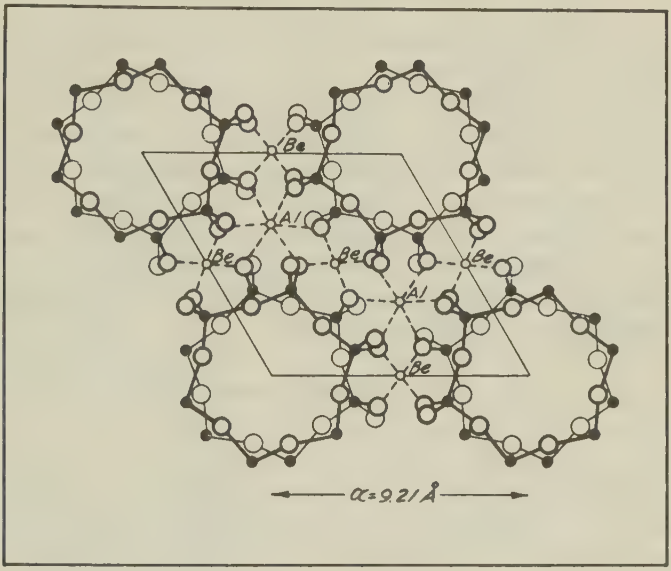

Fig. 2. The structure of beryl after Bragg and West (2, 3). The open hexagonal channels are the most striking feature of the structure.

The beryl-cordierite structure can accommodate variable amounts of the alkali ions Li, Na, and K (beryl may also contain Rb and Cs). The recorded range in alkali content is similar in the two minerals:

Beryl . . . 0.4 to 7.8 weight per cent alkalies (from 20 analyses).
Cordierite . . . 0.1 to 4.4 weight per cent alkalies (all recorded analyses).

The crystal habit of the two minerals is somewhat similar. Beryl occurs commonly as hexagonal prisms, cordierite as orthorhombic crystals cyclically twinned to a pseudo-hexagonal prism. Some beryl is orthorhombic and occurs as pseudo-hexagonal cyclic twins, identical with those of cordierite.

Beryl is normally uniaxial negative, but it may be biaxial with an optic angle (2E) up to 10°. Cordierite is usually biaxial with a wide range in optic angle. Tsuboi (20) reports a cordierite varying in optic angle from uniaxial positive to uniaxial negative within one crystal. Artificial iron-free cordierite may be uniaxial negative, like beryl (6). The indices likewise vary over an analogous range. Both minerals are dichroic; in beryl the dichroism is slight and variable, in most cordierite it is very strong.

ALKALIES IN THE CORDIERITE-BERYL STRUCTURE

In the preceding paragraphs establishing the relationship of cordierite and beryl, the alkali content was shown to vary over a similar range. Since the alkali ions have a very significant effect on the optical properties of beryl (Fig. 3) and, as will be shown, on cordierite, their position in the structure becomes a matter of some theoretical interest. The alkali ions have large ionic radii (Table 2), and, lithium and sodium excepted, cannot substitute for the smaller ions Be, Si, Al, Mg and Fe. It follows that the structure of beryl and cordierite must provide special accommodation for variable amounts of K, Rb and Cs (the larger alkali ions), without loss of structural stability.

TABLE 2. IONIC RADII OF THE ALKALI METALS

Li	0.78 Å
Na	0.98 Å
K	1.33 Å
Rb	1.49 Å
Cs	1.65 Å

The most striking features of the beryl structure are the hexagonal rings formed by six silicon oxygen tetrahedra (Fig. 2). To quote Bragg (3):

> These rings are stacked on each other along the hexagonal axis forming a series of open channels, for no atomic centre is nearer than 2.55 Å to a hexagonal axis. The whole structure is like a honeycomb with the hexagonal axes passing down the centres of the cells and within walls of closely packed oxygen atoms. The open channels in the structure are very striking and suggest investigation into properties they might confer on the crystal.

Bragg does not enlarge on this statement or discuss the structural relations of the alkali ions in beryl. His formulated structure is that of pure $Be_3Al_2Si_6O_{18}$ and he ignores the fact that beryl may contain up to 7.80% alkalies by weight.

Since K, Rb and Cs have such large ionic radii, the only available positions in the beryl structure are the hexagonal channels which Bragg mentions.

The possibility that the alkalies are located in these channels and the probable nature of the replacement which would necessarily accompany the introduction of positively charged ions were investigated by the writer for an alkali rich beryl (Table 3).

TABLE 3. IONS PRESENT IN ONE UNIT CELL OF CUSTER CO. BERYL*
Analyst R. E. Stevens (18)

Si		24.0
Fe		0.0
Be		8.3
Al		8.9
Na	1.23	3.0
Li	1.43	
K	0.11	
Rb	0.02	
Cs	0.23	
Ca		0.0
Mg		0.1
P		0.0
OH		6.0

Theoretically pure beryl	Be_{12}		$Al_8Si_{24}O_{72}$
Actual ions in Custer Co. beryl	Be_9	$Alk._3$	$Al_1Al_8Si_{24}O_{72}$
Proposed structural formulas			
(a) Custer Co. beryl	$(Na,K,Rb,Cs)_1Be_9$	$(Li, Na)_2$	$Al_1Al_8Si_{24}O_{72}$
(b) Alkali beryl in general	$(Alkalies)_xBe_{(12-2x)}$	$(Li, Na)_{2x}$	$Al_xAl_8Si_{24}O_{72}$

* The unit cell of beryl contains 24 silicon ions (4 molecules of $Be_3Al_2Si_6O_{18}$). Assuming the silicon content of each unit cell to be fixed at 24, the ionic ratios derived from the original analysis are recalculated into the number of ions in the unit cell by dividing each ratio by the number of unit cells statistically present. The following general equation is applied in making the recalculation:

$$\text{Number of ions in unit cell} = \text{Ionic ratio} \times \frac{24 \text{ (number Si ions in unit cell)}}{1054 \text{ (the ionic ratio of Si)}}\cdot$$

The nature of the substitution is therefore:

$$3 \text{ Alkali ions}^{+1} + 1 \text{ Al}^{+3} = 3 \text{ Be}^{+2}.$$

This substitution satisfies the structure electrostatically.

The probable position of the ions may be arrived at by comparing the cordierite structure with that of a conceivable alkali end member of the beryl series:

Pure beryl		Be_{12}		Al_8	Si_{24}		O_{72}
Alkali end member	$(Alkalies)_4$	$(Li, Na)_8$	Al_4	Al_8	Si_{24}		O_{72}
Cordierite		$(Fe, Mg)_8$	Al_4	Al_8	Si_{20}	Al_4	O_{72}

In cordierite four of the aluminum ions take four of the beryllium positions of beryl. This applies also to aluminum in the alkali end member of the beryl series, four of the beryllium positions being filled by aluminum ions.

The substitution of 8 magnesium ions in cordierite for the remaining 8 beryllium positions as postulated by Gossner and Mussgnug (8, 9) has an analogy in the alkali beryls. Magnesium has an ionic radius of .78 Å, identical with the ionic radius of lithium (.78 Å), slightly smaller than the ionic radius of sodium (.98 Å). Since magnesium (or iron) can take the position of the smaller ion beryllium without an essential change in the structure, it follows that 8 lithium and sodium ions can and do fill the remaining 8 beryllium positions of the alkali beryl.

The third alkali ion, needed for electrical stability in the alkali beryl structure, is in some of the unit cells cesium (1.65 Å), rubidium (1.49 Å) or potassium (1.33 Å), ions too large to substitute for beryllium. This third ion, then, must lie in one of the open hexagonal channels in the structure (Fig. 2).

It is felt that the substitution outlined above gives a very satisfactory explanation of the distribution of the alkali ions, and forms one more link in the chain of evidence relating the structures of beryl and cordierite.

Effect of Alkalies on the Optical Properties of Beryl

The intimate structural and optical relationship between cordierite and beryl has been established to validate an analogy between the effects of variable amounts of the alkalies on beryl and on cordierite.

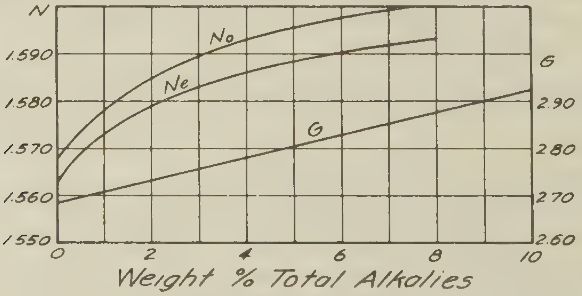

Fig. 3. The effect of alkalies on the optical and physical properties of beryl—after Winchell (22).

Figure 3 shows the effect of an increase in the alkali content on the properties of beryl, and from the figure inferences may be drawn as to the probable effect on cordierite.

An increase in alkali content in beryl is accompanied by:

(1) An increase in the indices.

(2) A change in the birefringence.

(3) The effect on the optical properties of any given increase in alkali content is greater for a low alkali beryl than for an alkali-rich beryl. It is not a straight line function like the increase in density with increasing alkalies.

EFFECT OF ALKALIES ON THE OPTICAL PROPERTIES OF CORDIERITE

By analogy with Fig. 3 an increase in alkali content in cordierite should:

(1) Increase the indices.
(2) Change the birefringence.
(3) Since cordierite is biaxial, change the optic angle.

The argument that the optical properties of cordierite are related in part to alkali content, to this point based on analogy, is confirmed by inductive reasoning based on actual analyses.

Unfortunately there are relatively few cordierite analyses in which the alkalies and calcium were determined. There are only fourteen complete analyses in the literature (Table 4) accompanied by sufficient optical data to use as evidence that the optical properties are determined in part by alkali and calcium content. The optical and chemical data are presented graphically in Figs. 4, 5, 6, 7, directly from this table.

TABLE 4. CORDIERITE—CHEMICAL ANALYSES AND OPTICAL PROPERTIES

Number	1	2	3	4	5
Author Occurrence	Pehrman Attu	Oppenheimer Twedestrand	Thiele Twedestrand	Thiele Orijarvi	Thiele Twedestrand
SiO_2	50.15	49.18	48.05	49.60	48.11
TiO_2	0.38	—	—	—	Trace
Al_2O_3	33.07	32.28	33.37	31.19	33.02
FeO	2.22	4.05	4.01	4.10	4.49
Fe_2O_3	1.52	0.08	0.09	1.19	0.81
MgO	11.01	11.25	11.11	11.13	10.95
MnO	0.12	—	Trace	—	0.07
Na_2O	0.14	0.21	0.26	0.21	0.12
K_2O	0.08	0.44	0.39	0.06	Trace
CaO	0.29	—	0.05	0.23	Trace
H_2O-	0.09	0.27	—	0.08	0.11
H_2O+	1.37	2.04	2.75	2.33	2.72
	100.44	99.80	100.08	100.22	100.16
% $Fe_2Al_4Si_5O_{18}$	15.7	17.0	17.1	20.4	21.2
Analyst	Pehrman	Dittrich	Thiele	Thiele	Thiele
Density	2.588	2.581	2.581	2.598	2.589
α	1.527	1.536	1.536	1.541	1.542
β	1.532	1.541	—	1.545	—
γ	1.538	1.543	1.543	1.547	1.548
2 V	92°	69° 26′	65° 36′	78° 12′	(74° 9′)
Optic sign	+	−	−	−	−

TABLE 4—*Continued*

Number	6	7	8	9	10
Author	Thiele	Oppenheimer	Thiele	Krishnan	Folinsbee
Occurrence	Bodenmais	Haddam	Langdorf	Madura	Great Slave
SiO_2	48.65	48.17	48.77	48.37	48.19
TiO_2	—	—	0.07	—	0.01
Al_2O_3	32.58	32.53	31.01	29.22	33.45
FeO	4.79	6.63	5.19	7.07	8.40
Fe_2O_3	1.75	1.21	2.83	2.20	0.55
MgO	10.02	8.86	8.91	9.54	7.95
MnO	—	—	0.31	0.42	0.18
Na_2O	0.15	1.39	0.16	—	0.22
K_2O	0.04	0.50	0.06	—	0.02
CaO	—	Trace	0.43	1.92	0.17
H_2O-	0.10	0.10	0.29	—	0.01
H_2O+	2.39	1.12	1.99	1.84	0.67
	100.26	100.51	100.02	100.58	99.82
% $Fe_2Al_4Si_5O_{18}$	26.2	32.3	33.3	35.6	39.0
Analyst	Thiele	Dittrich	Thiele	Krishnan	Folinsbee
Density	2.614	2.660	2.629	2.598	2.631
α	1.541	1.552	1.546	—	1.544
β	1.547	1.560	—	—	1.550
γ	1.550	1.561	1.558	—	1.556
2 V	(66° 24′)	43° 26′	—	85–99°	85–95°
Optic sign	−	−	−	±	±

TABLE 4—*Continued*

Number	11	12	13	14
Author	Thiele	Pehrman	Shibata	Shibata
Occurrence	Brocken	Ilmajoki	Dôsi	Sasago
SiO_2	48.88	50.09	43.55	43.27
TiO_2	—	0.00	—	—
Al_2O_3	33.07	31.78	30.68	30.25
FeO	8.05	8.71	13.17	15.31
Fe_2O_3	0.53	0.78	1.50	1.09
MgO	7.04	6.69	2.70	1.48
MnO	0.06	0.00	2.88	1.20
Na_2O	0.09	0.00	0.32	0.90
K_2O	—	0.07	1.32	3.53
CaO	0.04	0.00	0.16	0.10
H_2O-	0.20	—	—	—
H_2O+	2.21	1.43	3.72	2.89
	100.17	99.55	100.00	100.00
% $Fe_2Al_4Si_5O_{18}$	40.0	44.0	78.0	87.0
Analyst	Thiele	Pehrman	Tanaka	Tanaka
Density	2.647	2.650	2.72	2.75
α	1.549	1.543	1.555	1.558
β	(1.555)	1.548	1.566	1.568
γ	1.560	1.553	1.571	1.573
2 V	74° 36′	91° 29′	66°	68.5°
Optic sign	−	+	−	−

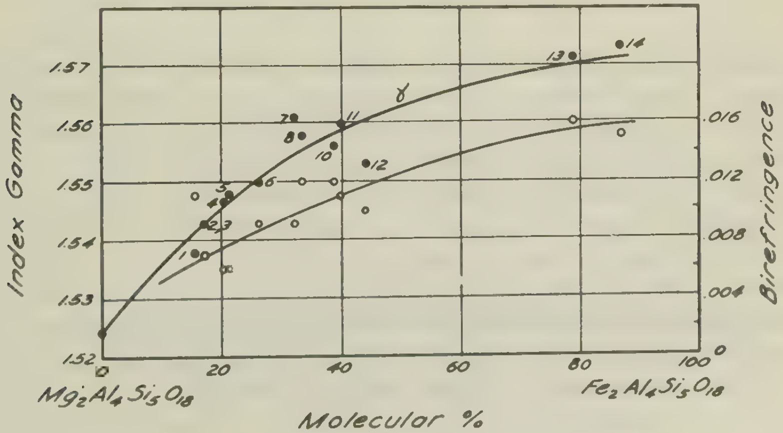

FIG. 4. The relation of index (upper curve) and birefringence (lower curve), in cordierite, to the Fe/Mg ratio.

Figure 4 shows clearly that an increase as in the Fe/Mg ratio increases the indices and birefringence of cordierite. The magnesian end member is a synthetic product (6).

The index of number 7 is anomalously high and it has a high alkali content. Numbers 1, 10, and 12 (anomalously low) are optically positive cordierite from the old shield areas. It is believed that their low index is a reflection of low alkali, high alkali-earth content.

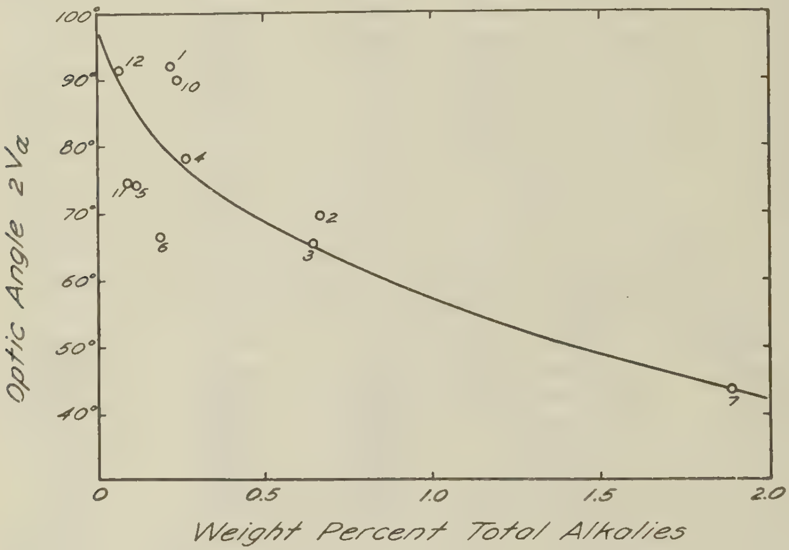

FIG. 5. The relation of optic angle in cordierite to the alkali content.

As indicated in Fig. 5 the optic angle in cordierite decreases with an increase in alkali content. Some of the points do not correspond closely with the curve, probably because of the effect of the variable CaO. Numbers 1 and 10 are high it is believed because of high CaO content. Numbers 11, 5 and 6 are low in CaO and therefore low in optic angle.

Numbers 13 and 14 (Table 4) are extremely iron-rich, alkali-rich cordierites. Their indices, birefringences and densities are very high, apparently related to the high iron content, possibly in part to the very high alkali content. They are not plotted on Figs. 5 or 7, and there are insufficient data to advance an explanation for their optic angles, other than that they belong to a distinct and rare group of the cordierite family.

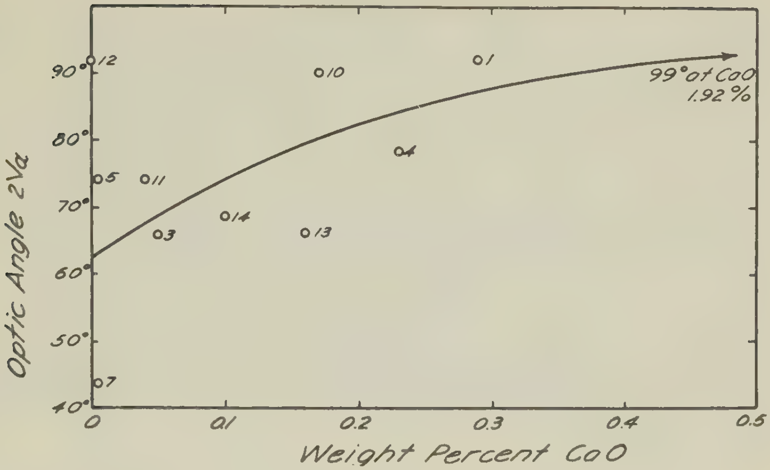

FIG. 6. The optic angle of cordierite tends to increase with an increase in CaO content.

An increase in the small amounts of CaO found in cordierite tends to increase the optic angle (Fig. 6). The anomalies arise from the subordination of the effect of CaO content to the effect of alkali content.

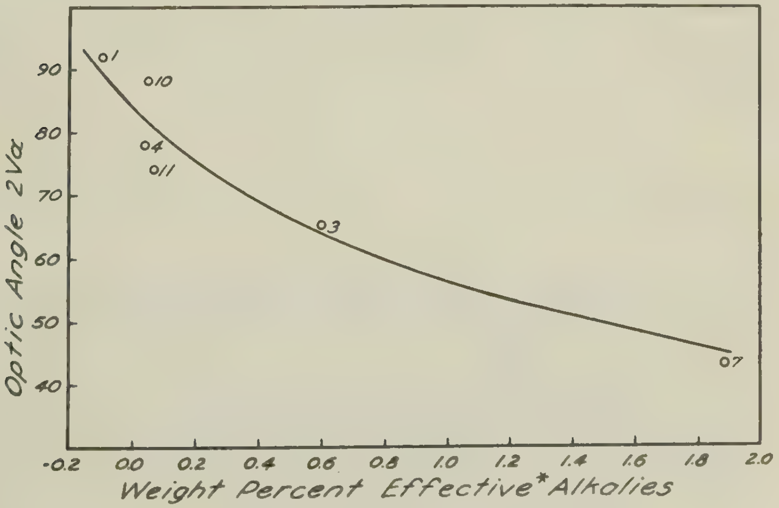

FIG. 7. The optic angle of cordierite plotted as a function of "effective" alkali content.

In Fig. 7 an attempt is made to eliminate the factor CaO in plotting the optic angle as a function of alkali content. The "effective" alkali content is arrived at by subtracting the weight percentage CaO from the weight percentage of total alkalies. Weight percentages are used in making this calculation rather than molecular percentages since optic properties in general are more nearly a function of density (weight percentage) than of number of ions (molecular percentage).

It is to be regretted that not all of the twelve analyses of Table 4 are complete. It is felt, however, that the graph establishes clearly the very close relation of effective alkali content and optic angle.

The effect of variables other than the per cent of $Fe_2Al_4Si_5O_{18}$, the alkalies, and the alkali earths should be considered. Thiele (19) in a recent paper presents seven new analyses and gives a very complete discussion of two variables hitherto unrecognized.

He is of the opinion:

(*a*) That an increase in water content affects the optic properties slightly, decreasing the indices and increasing the optic angle.

(*b*) That there may be an increase in the molecular percentage of silicon and magnesium as compared to aluminum due to isomorphous substitution of silicon and magnesium for aluminum.

$$Si^{+4}+Mg^{+2}=Al^{+3}+Al^{+3}$$

(*c*) That this substitution results in a decrease in indices and a sharp increase in the optic angle.

The writer cannot agree with these inferences of Thiele's after critical examination of the data upon which they were based.

SUMMARY AND CONCLUSIONS

The significant points brought out in this study of gem cordierite from the Great Slave Lake area are:

(1) A complete chemical analysis of cordierite from a new occurrence, especially significant since the analysis was made on selected fragments of exceptionally pure material, indicates that pure cordierite is very low in H_2O+.

(2) The analogy of the cordierite structure with that of beryl, as suggested by Gossner and Mussgnug on the basis of *x*-ray investigation is clarified by showing the close relationship of cordierite and beryl chemically, optically, and structurally.

(3) The nature of the isomorphous substitution accompanying the introduction of alkalies into the beryl structure is established for an alkali-rich beryl and confirmed by examination of the relation of the structural formulas of alkali beryl and cordierite.

(4) The Great Slave Lake cordierite is optically positive in character. The existence of optically positive cordierite has been questioned but the present results are carefully checked. A possible explanation of this anomaly is offered on the basis of a hitherto undiscussed variable in the chemical composition of cordierite—the alkali content.

(5) Alkalies have a pronounced effect on the optical properties of beryl, increasing the indices and birefringence. The variation in indices and birefringence of cordierite have previously been considered to be functions only of the Fe/Mg ratio (17, 21). The anomalies arising from this assumption are shown to be due to variations in the alkali content, the analogy between cordierite and beryl explaining the effects of this variable.

(6) An increase in the alkali content of cordierite is shown to:
Increase the indices.
Decrease the birefringence.
Lower the optic angle.

Optically positive cordierites are in general a group of cordierites comparatively low in alkalies and high in calcium.

This paper emphasizes the importance of complete chemical analyses. In making analyses all the common elements should be determined, even if present in small amounts. Rare elements also, whose presence might be indicated on the basis of mineral structure, should be determined. The ideal formula, arrived at by structural investigation, will then form a basis for distributing the atoms as determined by the chemical analysis (2).

Complete analyses are of enduring value in solving problems of mineral chemistry, optics, and physics. They solve not only an immediate problem, but may find useful application in future investigations.

ACKNOWLEDGMENTS

This study of the mineral cordierite embodies the principal findings of research leading to the degree of Master of Science at the University of Minnesota. The writer is very grateful to Professor F. F. Grout for considerate criticism and advice, to Dr. R. B. Ellestad of the rock analysis laboratory for supervision and assistance in making the analysis of cordierite, and to Professor J. W. Gruner for suggestions advanced on the structural aspects of the problem. The writer is indebted to the Geological Survey of Canada and to Drs. A. W. Jolliffe and C. S. Lord of the Survey for kind cooperation in the collection of the material, and to Dr. R. L. Rutherford of the University of Alberta for critical reading of the manuscript.

REFERENCES

1. BRAMMAL, A., AND RAO, B. R., The variable composition of cordierite from the Dartmoor granite: *Min. Mag.*, **24,** 254 (1936).
2. BRAGG, W. L., Atomic Structure of Minerals, New York, Cornell University Press, 37–40, 182–183 (**1937**).
3. BRAGG, W. L., AND WEST, J., The structure of beryl, $Be_3Al_2Si_6O_{18}$; *Proc. Roy. Soc. London*, Ser. A., **111,** 691–714 (1926).
4. CONANT, L. C., Optically positive cordierite from New Hampshire: *Am. Mineral.*, **20,** 310 (1935).
5. CHACKO, I. C., Optically positive cordierite: *Geol. Mag.*, **53,** 462–464 (1916).
6. DITTLER, E., AND KOHLER, A., Neue Beiträge zur Cordieritsynthese: *Centralbl. Mineralogie*, Abt. A. 149–159 (1938).
7. DOELTER, C., Cordierit: Handbuch der Mineralchemie, Band **11,** Teil 2, 614–627 (1917).
8. GOSSNER, B., Über structurelle Beziehungen zwischen Beryll und Cordierit: *Centralbl. Mineralogie*, Abt. A, 204–207 (**1928**).
9. GOSSNER, B., AND MUSSGNUG, F., Vergleichende röntgenographische Untersuchung von Magnesiumsilikaten: *Neues Jahrb. Mineral.*, Beilage-Band **58,** Abt. A, 216–227 (1928).
10. IYER, L. A. N., A study of the calc gneisses, scapolite gneisses and cordierite-garnet-sillimanite rocks of Madras: *Min. Mag.*, **22,** 121–135 (1929).
11. KRISHNAN, M. S., Notes on cordierite in a cordierite gneiss from Madura district, Madras, India: *Geol. Mag.*, **20,** 248–251 (1923–5).
12. OPPENHEIMER, L., Untersuchungen am Cordierit: *Verhandl. d. Heidelb. naturh.-med. Vereins.*, *N.F.* **13,** 257–302 (1914). Abstract: *Neues Jahrb. Mineral.*, Band **1,** 175–181 (1915).
13. PEHRMAN, G., Über optisch positiven Cordierit: *Acta Acad. Aboensis Math. et Physica*, **6,** 11 (1932). Abstract: *Neues Jahrb. Mineral.*, Referate **1,** 358–359 (1934).
14. READ, H. H., Occurrence of iron-rich cordierite in Aberdeenshire: *Geol. Mag.*, **66,** 547–552 (1929).
15. RUTHERFORD, R. L., Optically positive cordierite in the Kisseyenew gneiss at Sherridon, Manitoba: *Am. Mineral.*, **21,** 386–388 (1936).
16. RUTHERFORD, R. L., Optically positive cordierite from the Northwest Territories, Canada: *Am. Mineral.*, **18,** 216 (1933).
17. SHIBATA, H., Graphic intergrowth of cordierite and quartz in pegmatites from Sasago and Dosi, Province of Kai, Japan: *Jap. Jour. Geol. and Geography*, **13,** 205–229 (1936).
18. STEVENS, R. E., Beryl-slightly altered material from Custer Co., South Dakota: *U. S. Geol. Survey, Bull.* **878,** 99.
19. THIELE, E., Die Beziehung der chemischen Zusammensetzung zu den physikalisch-optischen Eigenschaften in einigen Mineralien des Kontakts: *Chemie der Erde*, **13,** 64–91 (1940).
20. TSUBOI, S., Whole range variation of the optical angle in cordierite from Sakumamura, Iwata-gori, Siduoka Prefecture: *Jap. Jour. Geol. and Geography*, **13,** 337 (1936).
21. WINCHELL, A. N., Cordierite: *Am. Mineral.*, **22,** 1175–1179 (1937).
22. WINCHELL, A. N., Elements of Optical Mineralogy, Part II, New York, John Wiley and Sons, 212–213 (**1933**).

COLUMBOMICROLITE FROM ESHOWE, NATAL

J. E. de Villiers, *Geological Survey of the Union of South Africa, Pretoria.*

Abstract

Columbomicrolite, a new member of the pyrochlore group occurring as tiny grains in albitite, has the following composition (recalculated to 100%): Cb_2O_5 72.2%, Ta_2O_5 nil, TiO_2 1.8%, Fe_2O_3 trace, Ce_2O_3 nil, CaO 15.2%, Na_2O 10.0%, H_2O 1.8%. Total 100.0%. $G.=4.16$. $n=2.152$. A brief summary is given of what is regarded as the essential chemical character of each member of the group.

Occurrence

While examining a rock sample from Natal during 1938, the writer observed a few grains of a highly refracting, isotropic mineral in the heavy concentrate. Its optical properties closely resembled those of diamond but chemical tests on a micro-scale showed the presence of columbium. At a later date more of the material was obtained and the mineral provisionally identified as microlite.

The parent rock is a somewhat weathered albitite which, according to Dr. Willemse of the Geological Survey, occurs in the Basement gneiss about fifteen miles north of the village of Eshowe. The rock usually has a sugary texture, but may also be lamellar or platy. Subordinate amounts of potash feldspar and muscovite are present and the latter mineral also occurs as veinlets traversing the specimens. It seems likely that the albitite has resulted from post-magmatic activity.

The specimens investigated did not contain a great variety of heavy minerals, and apart from the columbomicrolite only ilmenite and zircon were present in appreciable amounts. Columbomicrolite is distributed through this rock in small, variable amounts, the highest percentage recovered being .05%.

The mineral was extracted by crushing and panning the rock and separating the concentrate by means of bromoform. Ilmenite was removed with the electromagnet, leaving a mixture composed exclusively of columbomicrolite and zircon.

Physical Properties

Grains of columbomicrolite are typically colorless and transparent, but are in part also somewhat turbid. Tiny films and flakes of a reddish translucent mineral, which may be hematite, are sometimes present as inclusions. In thin sections of the rock, columbomicrolite was observed in a few cases. It forms small patches and irregular vein-like structures made up of individual crystals that showed some tendency toward idiomorphic outline. The aggregates are up to 0.2 mm. in diameter, while individual crystals have a cross section of the order of 0.05 mm.

A specific gravity determination made on about 200 milligrams of the mixture of columbomicrolite and zircon, using a small, specially made pycnometer, gave the following result: $G=4.33$. Correcting this figure for the presence of 37% zircon with a specific gravity of 4.65, the result for columbomicrolite was found to be 4.16. The zircon has normal refractive indices but it shows some signs of alteration and it is thus likely that its assumed specific gravity is too high. The figure for columbomicrolite cannot be considered as more than an approximation and may have an error of ±.1.

The refractive index was determined by immersion in sulphur-selenium melts. These melts were prepared by heating together the constituents in a test tube to a temperature near to the boiling point of sulphur and then pouring the product into a cool dish. A small fragment of this elastic material was next placed on a glass slide together with a few grains of columbomicrolite, covered with a small cover glass and heated until melting just took place. The melt after being quickly cooled on a metal slab proved to be fairly transparent and remained amorphous long enough for index determinations to be made. This method, whereby the mixture does not need to be heated to a high temperature in the presence of the mineral, has the advantage that the mineral is less likely to suffer a change of index through heating. It has indeed been found possible to make mounts of a mineral in the elastic medium in the cold. These mounts were not, however, very satisfactory.

The composition of the mixture was altered until its index matched that of the mineral for sodium light. Another portion of the same mixture was then pressed into a glass prism and its refractive index determined on the goniometer. The refractive index of columbomicrolite obtained in this way gave the result: $n_D=2.152$ ($\pm.005$). No marked differences in index were observed among individual grains, a fact which indicates that the mineral is of fairly uniform composition.

CHEMICAL PROPERTIES

About 350 milligrams of the mixture of columbomicrolite and zircon were kindly analyzed by Mr. C. F. J. van der Walt of the Division of Chemical Services. Mr. van der Walt's report is given below:

"Loss on ignition was taken to be H_2O. The material was decomposed with HF and then fumed with H_2SO_4 to remove all HF. The earth acids plus zircon were filtered off and the CaO and Na_2O were determined according to the usual methods in the filtrate after the metals of the ammonia group had been removed (CaO was determined according to the oxalate method, and the Na_2O by weighing as Na_2SO_4).

"The insoluble residue (earth acids plus zircon) was fused with $K_2S_2O_7$, taken up in tartaric acid solution and filtered. The earth acids were now precipitated from the filtrate according to the tartaric hydrolysis method of Schoeller, weighed and tested for tantalum according to the tannic acid method of Schoeller. Tantalum was found to be absent, as no yellow precipitate could be obtained. The precipitate was red from the start, showing that only columbium was present.

Analytical Data

	1	2	3	4	5	6
	%	%				
Cb_2O_5	43.5	71.2	0.267	0.535	0.535	71.3
Ta_2O_5	nil					
TiO_2	1.1	1.8	0.023	0.023	0.023	1.8
Fe_2O_3	tr.					
Ce_2O_3	nil					
CaO	9.3	15.2	0.271	0.271	0.271	15.2
Na_2O	6.1	10.0	0.161	0.322	0.287	8.9
H_2O	1.1	1.8	0.100	0.200	0.310	2.8
Insol.	36.9					
	98.0	100.0				100.0

1. Analysis by C. F. J. van der Walt.
2. Analysis of columbomicrolite recalculated to 100%.
3. Molecular ratios.
4. Atomic ratios.
5. Atomic ratios adjusted to conform to the formula $(Ca, Na)_2(Cb, Ti)_2(O, OH)_7$.
6. Theoretical composition for Ca=0.97, Na=1.03, Cb=1.92, Ti=0.08, O=5.89, OH=1.11.

"The insoluble residue (zircon) was determined by fusing a fresh sample with $K_2S_2O_7$ and dissolving in tartaric acid. The residue was ignited and weighed. The TiO_2 was determined colorimetrically in the filtrate.

"The percentage of insoluble residue (zircon) is slightly low, because zircon is slowly attached by $K_2S_2O_7$, so that some zirconium found its way into solution, and is not accounted for in the analysis.

"A test was made for rare earths by means of oxalic acid. No precipitate was obtained."

The agreement between the recalculated analysis and the theoretical composition for a mineral of the pyrochlore type will be seen by comparing columns 2 and 6. Discrepancies in the soda and water values are rather large (±1% in either case) but when it is borne in mind that the analysis was carried out on very little material the agreement must be considered satisfactory.

The molecular weight calculated from the theoretical composition was found to be 358. Von Gaertner (1930) has stated that the unit cell of pyrochlore contains 8 molecules of the type $(Na, Ca)_2 (Nb, Ti)_2 (O, F)_7$. With this information and the specific gravity, the edge of the cubic unit cell of columbomicrolite may be calculated. The value obtained (10.43Å) agrees closely with Machatschki's (1932,*b*) determinations on minerals of the pyrochlore-romeite group.

NOMENCLATURE OF THE PYROCHLORE GROUP

No suitable name for the Eschowe mineral could be found in relevant literature. Indeed, considerable confusion seemed to exist in regard to the definitions applied to the various members of the pyrochlore group. It was thus thought necessary to undertake a survey of these minerals and to apply to each a brief definition which would be in accord with its known composition and properties, and would enable any member of the group to be identified by means of a qualitative chemical analysis in conjunction with optical and physical tests.

All the minerals for which definitions are proposed (except "marignacite" which is described as a variety of pyrochlore; and columbomicrolite) have been investigated with the aid of *x*-rays by Machatschki (1832,*b*) and others. They belong to the pyrochlore group and have the general formula $X_2Z_2(O, OH, F)_7$, where $X = Na, Ca, Ce$, etc., and $Z = Nb, Ta, Ti, Sb$. Unfortunately, the writer has not been able to obtain Machatschki's publication and has had to be content with abstracts.

In determining which constituents should be considered diagnostic for any species, it was decided to emphasize where possible the presence of elements unique to such a species and to give less consideration to constituents like sodium, iron, water, fluorine, etc., which are very often present and usually in subordinate amounts.

Pyrochlore. Wöhler, *Pogg.*, **7,** 417 (1826). Larsen and Berman (1934) define pyrochlore as a "Columbate and titanate of Ce, Ca, etc., with Th, F, etc.," while Winchell (1933) gives the following formula (after Machatschki, 1932,*b*): $(Na, Ca, Fe, Ce)_2 Nb_2O_6 (OH, F)$. A study of the available analyses of pyrochlore shows that both cerium and titanium are invariably present in appreciable amounts and must therefore be regarded as essential constituents. From a consideration of these facts the mineral can be shortly defined as a calcium-cerium titano-columbate which usually, but not necessarily, contains iron and sodium and small amounts of fluorine, water, etc.

Microlite. C. U. Shepard, *Am. Jour. Sci.*, **27,** 361 (1835). It appears to be generally accepted that this mineral is chiefly a calcium tantalate. Sodium and water are usually present but are not considered essential.

Columbomicrolite. This mineral can be defined as a calcium columbate ($Ca_2Cb_2O_7$) which in the case of the Eschowe mineral also contains sodium and water.

Hatchettolite. J. L. Smith, *Am. Jour. Sci.*, **13,** 365 (1877). A tantalo-columbate of uranium and calcium, which may contain small amounts of iron, water, titanium, etc. Uranium is considered to be the significant constituent of this species and it is proposed that any uranium-rich pyrochlore be named hatchettolite. Microlite containing much uranium may be named tantalohatchettolite.

Koppite. Knop, *Jb. Min.*, **67,** (1875). Winchell (1933) describes this mineral as "a pyrochlore containing K" while Brandenberger (1931) states that koppite should be regarded as an iron-columbium pyrochlore. From an examination of the available analyses of koppite it must however be concluded that the significant difference between this mineral and pyrochlore lies in the absence of appreciable amounts of titanium in koppite. The mineral can thus be defined as a calcium-cerium columbate which may, or may not, contain accessory iron, sodium potassium, etc.

Weidman and Lenher's marignacite, *Am. Jour. Sci.*, **23,** 287 (1907), which contains only 2.88% TiO_2 should, according to this definition, also be named koppite.

Pyrrhite. G. Rose, *Pogg.*, **48,** 562 (1840). Information on the composition of this mineral is very scanty. A partial analysis by Brauns (quoted by Machatschki, 1932,*a*) showed the presence of characteristic pyrochlore constituents and Machatschki (1932,*a*) describes the mineral as a tantalum-rich member of the pyrochlore series. Since no differences between pyrrhite and pyrochlore are apparent, it is proposed that the former name be discarded in favor of the latter which has priority.

Neotantalite. Pierre Termier, *Bull. Soc. Min.*, **25,** 34 (1902). This mineral was assigned to the pyrochlore group by Machatschki (1932,*b*) who proposed the formula $(Fe, Mn, Na)_2\ (Ta, Cb)_2\ (O, OH, F)_7$. Pisani's analysis however shows little correspondence to a formula of this type. In view of this lack of agreement it seems advisable for the present to use the name neotantalite only in referring to the type mineral.

Romeite. Damour, *Ann. Mines*, **20,** 247 (1841). Calcium antimonate ($Ca_2Sb_2O_7$) usually containing small amounts of sodium, manganese, iron and water.

Atopite. A. E. Nordenskiold, *Geol. För. Förh.*, **3,** 376 (1877). Similar in composition to romeite. O. Zeidlitz (1932) has suggested that the name atopite be abandoned in favor of romeite which has priority.

Schneebergite. A. Brezina, *Vh. G. Reichs.*, 313 (1880). A calcium antimonate to which Schaller (1916,*a*) assigns the empirical formula $CaSbO_3$ ($=2CaO\cdot Sb_2O_3+2CaO\cdot Sb_2O_5$). Zedlitz (1932) has however shown the mineral to be isomorphous with romeite. There thus seems to be no reason why the name schneebergite should be retained and it is proposed that the name romeite be substituted for this.

Lewisite. E. Hussak and G. T. Prior, *Min. Mag.*, **11**, 80 (1895). Calcium titano-antimonate which may contain small amounts of iron, sodium and manganese.

Mauzeliite. H. Sjögren, *Geol. För. Förh.*, **17**, 313 (1895). Schaller (1916,*b*) considers the mineral to be identical with lewisite and there seems to be some room for doubt as to whether the name should be retained. In view however of the presence of 6.79% PbO in the original analysis it is suggested that the name mauzeliite be used to describe a calcium-lead titano-antimonate.

Monimolite. L. J. Igelström, *Öfv. Ak. Stockh.*, **22**, 227 (1865). Lead antimonate with or without calcium, iron, magnesium, etc.

Weslienite. G. Flink, *Geol. För. Förh.*, **45**, 567 (1923). Calcium antimonate of similar composition to romeite. Aminoff (1933) states that the mineral is identical with atopite and it is therefore proposed that the name weslienite be discarded in favor of romeite.

REFERENCES

AMINOFF, G., On the minerals "weslienite" and atopite: *Kungl. Svenska Vetenskapsakad. Handl.*, ser. 3, **11**, no. 4, 14–18 (1933).

BRANDENBERGER, E., Die Kristallstruktur von Koppit: *Zeits. Krist.*, **76**, 322–334 (1931).

LARSEN, E. S., AND BERMAN, H., The Microscopic Determination of Nonopaque Minerals: *U. S. Geol. Surv., Bull.* **848** (1934).

a. MACHATSCHKI, F., Die Kristallstruktur des Pyrrhit: *Centr. Min.*, Abt. A, 33–37 (1932).

b. MACHATSCHKI, F., Die Pyrochlor-Romeit Gruppe: *Chemie der Erde*, **7**, 56–76 (1932).

PALACHE, C., AND GONYER, F. A., Microlite and stibiotantalite from Topsham, Maine: *Am. Mineral.*, **25**, 411–417 (1940).

a. SCHALLER, W. T., Schneebergite: *Min. Notes, Ser. 3, U. S. Geol. Surv., Bull.* **610**, 81–94 (1916).

b. SCHALLER, W. T., The natural antimonites and antimonates: *Min. Notes, Ser. 3, U. S. Geol. Surv., Bull.* **610**, 104–105 (1916).

VON GAERTNER, H. R., Die Kristallstrukturen von Loparit und Pyrochlor: *Neues Jahrb. Min.*, Abt. A, Beil.-Bd. **61**, 1–30 (1930).

WINCHELL, A. N., Elements of Optical Mineralogy, Part II (1933).

ZEDLITZ, O., Die Kristallstrukturen von Romeit und Schneebergit: *Zeits. Krist.*, **81**, 253–263 (1932).

NOTES AND NEWS

THE ROWE COLLECTION

Albert S. Wilkerson,
Rutgers University, New Brunswick, New Jersey.

Last October Rutgers University was the recipient of a locally well-known collection of minerals. The donor was Mr. George Rowe of Rowe Place, Franklin, New Jersey. The Rowe Collection is now on display in the Museum of Geological Hall, Rutgers University. The Collection is of interest because of its many rare minerals and the large number of Franklin mineral species.

George Rowe was born in Cornwall, England, in 1868. At the age of eleven years he started to work in the mines near his home. He came to the United States when he was eighteen years old, and obtained employment in the iron mines of Michigan and Minnesota. In 1906 Rowe became identified with the New Jersey Zinc Company of Franklin, New Jersey. Rowe was mine captain from 1906 until 1937, when he retired.

Although not a trained mineralogist, Rowe possessed a keen eye for rare crystal forms and rare minerals. Most of the specimens in the Collection were found by Rowe, although many were given to him by his associates, and a few were purchased from mineral dealers.

Many of the rare minerals were identified by L. H. Bauer of the chemical laboratory of the New Jersey Zinc Company at Franklin, and by Dr. Charles Palache. Palache[1] acknowledges the Rowe Collection as one of the collections that furnished valuable data for his study of Franklin minerals.

Approximately 2400 specimens, consisting of 246 mineral species and varieties, make up the Collection. Thirty States and 26 foreign countries are represented. About half of the specimens are from New Jersey, 931 from Franklin. Of the 151 known species from Franklin, 129 are in the Collection. Roweite—a light brown, lath-shaped orthorhombic mineral, 5 in hardness, a hydrous borate of manganese and calcium—will soon be added. Mr. Rowe owns one of the three specimens named in his honor and has stated his intention of giving it to Rutgers.

Following is a summary of the more rare species and varieities in the collection, the common minerals being omitted:

---

[1] Palache, Charles: *U. S. Geol. Survey, Prof. Paper* **180,** 2 (1937).

Allactite; Franklin
Allanite; Franklin
Ammiolite; Chile
Anomite; Franklin
Autunite; Bedford, N. Y.
Barylite; Franklin
Barysilite; Franklin
Bayldonite; Cornwall, England
Cahnite; Franklin
Calcium larsenite; Franklin
Caswellite; Franklin
Chalcophanite; Franklin
Chlorophoenicite; Franklin
Cleiophane; Franklin
Clinoclasite; Tintic, Utah
Clinohedrite; Franklin
Coccolite; Franklin
Colerainite; Chester Co., Pa.
Cummingtonite; Franklin
Cyprine; Franklin
Diabantite; Paterson, N. J.
Edenite; Franklin
Ellsworthite; Hybla, Ontario
Epidesmine; Montgomery Co., Pa.
Fizelyite; Hungary
Fluoborite; Franklin
Fowlerite; Franklin
Franklinite; Franklin
Friedelite; Franklin
Gageite; Franklin
Gahnite; Franklin
Ganophyllite; Franklin
Geocronite; Sala, Sweden
Glockerite; Philadelphia, Pa.
Greenockite; Franklin
Hancockite; Franklin
Hardystonite; Franklin
Hedyphane; Franklin
Herderite; Poland, Me.
Hetaerolite; Franklin
Hodgkinsonite; Franklin
Hydrohetaerolite; Franklin
Jeffersonite; Franklin
Jossaite; Beresof, Siberia
Jordanite; Binnenthal, Switzerland
Keilhauite; Arundal, Norway
Larsenite; Franklin
Lead; Franklin
Leucophoenicite; Franklin
Linarite; Osani, S.W. Africa
Lithiophilite; Branchville, Conn.
Manganosite; Franklin
Margarosanite; Franklin
McGovernite; Stirling Hill, N. J.
Nasonite; Franklin
Norbergite; Franklin
Pyrochroite; Franklin
Roeblingite; Franklin
Roepperite; Ogdensburg, N. J.
Schorlomite; Magnet Cove, Ark.
Schallerite; Franklin
Schefferite; Franklin
Sussexite; Franklin
Triploidite; Conn.
Vonsenite; Riverside, Calif.
Vauxemite; Franklin
Voquelinite; Beresof, Siberia
Vorhauserite; Franklin
Willemite; Franklin
Xonotlite; Franklin
Zincite; Franklin
Zunyite; Zuny Mine, Col.

Of interest is a single specimen of yellow spinel embedded in Franklin limestone, presenting the form of a simple cube modified by a trace of the octahedron. It is unique among Franklin spinel specimens and has received special mention by Palache.

Sixty-one rhodonite specimens of various shades, dimensions, and complexity of crystal forms is the outstanding feature of the Collection.

More than a hundred specimens are fluorescent, some phosphorescent.

IDOCRASE AND SCAPOLITE FROM MANCHESTER, NEW HAMPSHIRE

Glenn W. Stewart,
Purdue University, Lafayette, Indiana.

Introduction

During the excavation for the National Guard Armory at Manchester, New Hampshire, in the spring of 1939, bedrock was exposed in several places. In one of the outcrops on the south side of the property, John E. Warren, of Manchester, found some interesting and colorful minerals which were identified as idocrase, scapolite, and garnet. This deposit was visited by Dr. George W. White, of the Geology Department at the University of New Hampshire, and the author during the summer of 1939.

The bedrock is a biotite schist with small and narrow calcareous bands interbedded with lenses of coarse granite and simple pegmatites. The schistocity of these rock units has a regional east-west dip. Some of the calcareous bands, in which the idocrase and garnet are located, display alternating red and brown colors. Frequently, a green band is present due to abundant diopside. Hitchcock (1) in his discussion of the bedrock of the Manchester area states that, "I have occasionally seen limestone seams two inches wide in the gneiss."

The author wishes to express his appreciation to Mrs. G. I. Hopkins, of Manchester, New Hampshire, for the use of several excellent specimens collected from this deposit.

Idocrase and Garnet

Idocrase usually occurs in irregular masses and bands throughout the calcareous seams, but an occasional crystal is found embedded in calcite or in small cavities where it is associated with garnets. The idocrase crystals that are present with the garnets are developed in columnar aggregates ranging from two to four millimeters in diameter, and have a greenish-brown color. Growth along the *c*-axis seems to have been suppressed somewhat and many of the crystals are rather stubby, six millimeters in length or less. Figure 1 illustrates a crystal of this type.

In contrast to the idocrase of the cavity a small isolated crystal of idocrase embedded in calcite has well developed $m\{110\}$ and $e\ \{101\}$ faces and a small elongated base, $c\ \{001\}$. The crystal was not removed from the calcite, but it appears to have duplicate faces on the other side. This crystal is illustrated in Fig. 2 and is six millimeters along the *c*-axis.

The indices of refraction for this unanalyzed idocrase determined by the immersion method with white light are: $\omega = 1.730 \pm .001$, $\epsilon = 1.719 \pm .001$.

Garnet, variety grossularite, $n = 1.755 \pm .002$, is rather abundant in the crystalline masses and in the cavities described above where their habit is dodecahedral. The individual reddish-brown crystals range from two to twenty millimeters in diameter. Several of the smaller crystals display both dodecahedral and trapezohedral faces.

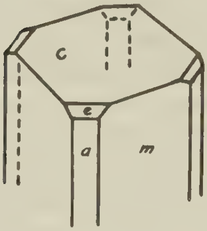

FIG. 1. Idocrase.

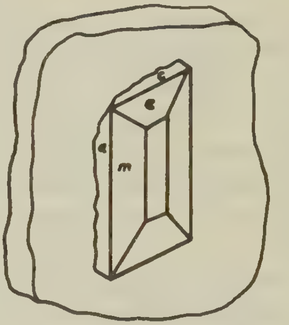

FIG. 2. Idocrase embedded in calcite.

One prism of dark green diopside was found which shows prominent $m\{110\}$ and $a\{100\}$ faces. Masses of diopside crystals are abundant and occur in green bands associated with the idocrase and garnet.

SCAPOLITE (MIZZONITE)

Scapolite occurs in irregular columnar masses and is usually found replacing quartz. No complete crystals were found, but crystalline aggregates suggest a tetragonal form and prismatic $m\{110\}$ faces can be seen. The mineral is white, has a subvitreous to vitreous luster, and a specific gravity of 2.69. Striations are present on the prism faces, and parallel the direction of the c-axis. The indices of refraction determined by the immersion method with white light are: $\omega = 1.591 \pm .001$, $\epsilon = 1.557 \pm .001$.

The chemical analysis by G. Barthauer, of Purdue University, shows a Ca/Na ratio of 73.4/26.6. This ratio, along with the indices of refraction, seem to place the mineral in the mizzonite range of the scapolite series. The spectroscopic analysis showed traces of iron, titanium, and manganese.

ANALYSIS OF SCAPOLITE (MIZZONITE)

SiO_2	46.78
Fe_2O_3	0.22
CaO	17.98
Al_2O_3	28.53
MgO	0.25
K_2O	0.06
Na_2O	6.50
Total (dry basis)	100.32

Summary

This deposit of idocrase is very similar in its general appearance, mineral association, and structural relationships to that of Center Strafford, New Hampshire, described by the author (2). Most of the minerals occur in the same proportions except that there is abundant scapolite in the Manchester deposit and none at Center Strafford. This contrast might possibly be due to larger calcareous seams which would furnish calcium for the scapolite. There seems to be little evidence of an introduction, or presence, of potash at Manchester as compared to the orthoclase (adularia) at Center Strafford.

The mineral associations and adjoining granitic lenses are suggestive of local contact metamorphism of calcareous sediments, probably calcareous sandstone.

References

1. Hitchcock, C. H., The Geology of New Hampshire: **2,** 554 (1874–1878).
2. Stewart, Glenn W., Vesuvianite and fluorescent apatite from Center Strafford, New Hampshire: *Am. Mineral.*, **24,** 274–275 (1939).

OCCURRENCE OF MARTITE IN MICACEOUS HEMATITE NEAR ESMONT, VIRGINIA

A. A. Pegau and W. C. Overstreet*

The senior author found some octahedra in certain specimens of a micaceous hematite presented to him for examination. At first he thought they might be magnetite, but since they were only slightly magnetic he suspected them to be martite, and turned them over to the junior author for a more detailed examination.

The martite occurs as octahedra disseminated through a dark steel-gray micaceous hematite which occurs near Esmont, Virginia.

In size the octahedra varied from 2 mm. to 7 mm. along a crystallographic axis, and in weight they ranged from about 50 milligrams to 330 milligrams. Some of the octahedra were perfectly developed, but most showed a distinct shortening along at least one axis.

The faces of the form showed minute pitting and also the impressions of smaller octahedra. The physical properties of the mineral include: octahedral crystallization, spinel twinning, $G=5.1$, $H=6$, submetallic luster, dark steel-gray color with bronze tarnish, reddish brown streak, conchoidal fracture, and feeble magnetism.

About 15% of the crystals examined showed no magnetism; others varied from feebly to strongly magnetic.

Both ferrous and ferric iron were found, with ferric iron the more abundant. The amount of ferrous iron obtained from the nonmagnetic specimens was appreciably less than the amount found in the magnetic crystals.

The authors are of the opinion that this mineral is martite, resulting from the pseudomorphous replacement of magnetite. The presence of ferrous iron and the pitted surface of the octahedra are taken as evidence of incomplete replacement. The red streak from a fresh surface of the mineral likewise suggests martite.

It is believed that this is the first report of martite from the State of Virginia.

---

* Published with the permission of the Virginia State Geological Survey.

PROCEEDINGS OF SOCIETIES

PHILADELPHIA MINERALOGICAL SOCIETY

The Academy of Natural Sciences of Philadelphia, March 6, 1941.

Dr. Thomas presided, with 58 members and visitors present. Dr. Michael Fleischer of the U. S. Geological Survey addressed the society on "The Role of Hydrogen in Minerals." Pressure-temperature data are obtained by carefully controlled heating methods and the results are plotted. An x-ray analysis will reveal the possibility of the water being either a part of the structural lattice or merely adsorbed. There is a great variance in the amount of energy that binds the hydroxyl to the crystal lattice. Interlayered water will cause minerals such as bentonite to expand along the c-axis on heating, without changing the lattice.

FORREST L. LENKER, *Secretary*

Academy of Natural Sciences of Philadelphia, April 3, 1941.

President W. Hersey Thomas presided with 64 members and visitors attending.

Dr. A. F. Buddington of Princeton University was the speaker of the evening, his subject was "Mineral Specimen Localities of the Adirondacks, with Special Reference to their Genesis." He described the work done by William Agar and himself some years ago in relocating some of the deposits with the aid of the notes of C. D. Nimms, a mineral collector of the late 19th century.

Dr. Buddington described briefly the general geology of the area—Grenville sediments, mostly limestones intruded by granites and syenites, the well crystallized minerals occurring at or near the igneous rock contacts with limestone. The mineral associations, with apatite, tourmaline, danburite and others containing various volatile elements, show that emanations from the cooling igneous rocks were largely responsible for most of the mineralization.

One purpose of this study was the determination of the temperatures of the granitic and syenitic magmas at the time of their intrusion. This was accomplished by noting the character of the metamorphic minerals in their vicinity. At the granite-limestone contacts were developed: garnet, microcline, albite, tremolite, brown tourmaline, pale pyroxenes, and scapolites of the marialite-mizzonite range. At the syenite-limestone contacts are found: perthite, wollastonite, dark pyroxenes, and scapolites of the wenerite-meionite range. These mineral associations indicate that the syenite magma was of higher temperature than the granite magma.

Dr. Buddington took up the description of the individual mineral localities in order of their temperature of formation. Zoning of the ore-deposits according to temperature stability ranges of their minerals is quite conspicuous in the area. For instance, the magnetite deposits of Port Henry and Lyon Mountains are limited to the granite core. All of the iron was precipitated from the late hydrothermal solutions before these reached the surrounding limestones. However, the core was too hot for the precipitation of lead and zinc minerals, so these entered and replaced the limestones, as at Edwards and Balmat.

The Balmat deposit presents many interesting problems. In the Grenville limestone are found halite, and anhydrite. These suggest the possibility of interbedded halite and anhydrite of Archean age. Methane gas is also present in the workings, suggesting the presence of organic material. Also present are secondary sphalerite, willemite, hematite, ilvaite, and chlorite. These seem to be due to groundwater alterations and were attributed by the speaker to downward penetrations of groundwaters from a surface exposed before the deposition of the Cambrian Potsdam sediments, roughly one half billion years ago. He attributes the hematite deposits of the Antwerp type to the alteration of gossans formed before the deposition of the Potsdam, which preserved them until the present. Where the protective coating of sandstone had been eroded from pyritic shales, only small limonitic gossans are found.

At higher temperatures silica-bearing solutions reacted with dolomitic beds in the limestone-forming tremolite. As temperatures dropped some of the tremolite was altered to talc forming deposits of economic value, as that near Edwards. Some of the manganese tremolite, hexagonite, is found here.

Black iron-bearing tourmaline such as is found at Pierpont is limited to the pegmatites, whereas the brown magnesium tourmaline, which is found near Gouverneur, is limited to the limestones, showing again that the iron was not able to leave the warm igneous rocks.

The speaker gave his views on the origin of the garnets of the Gore Mountain deposit. The ordinary gabbro of the Adirondacks suffered compression from mountain building forces at a temperature of about 600°C. in the presence of chlorine, which favored migration of the constituent elements. At first garnet formed a rim between grains of hypersthene in contact with labradorite, and the pyroxene was changed to augite. Where the reaction went to completion under favorable conditions, concretionary garnets formed, leaving the surrounding minerals purified of garnet constituents. Since the garnets grew under stress, they now have a well defined jointing which causes them to break into sharp angular fragments favoring their use as abrasives.

Dr. Buddington illustrated his discussion with lantern slides and answered many pertinent questions.

Louis Moyd, *Acting Secretary.*

Dr. Olaf Andersen, professor of petrographic analysis at the Stevens Institute of Technology, died on July 18 at the age of fifty-seven years.